IEEE Access
Multidisciplinary | Rapid Review | Open Access Journal

Received 5 July 2022, accepted 16 July 2022, date of publication 26 July 2022, date of current version 15 August 2022.

Digital Object Identifier 10.1109/ACCESS.2022.3194050

SURVEY

Position, Navigation, and Timing (PNT) Through Low Earth Orbit (LEO) Satellites: A Survey on Current Status, Challenges, and Opportunities

F. S. PROL[1], R. MORALES FERRE[2], Z. SALEEM[3], (Graduate Student Member, IEEE), P. VÄLISUO[4], C. PINELL[1], E. S. LOHAN[2], (Senior Member, IEEE), M. ELSANHOURY[4], (Graduate Student Member, IEEE), M. ELMUSRATI[4], (Senior Member, IEEE), S. ISLAM[1], K. ÇELIKBILEK[2], K. SELVAN[4], J. YLIAHO[5], K. RUTLEDGE[4], A. OJALA[6], L. FERRANTI[3,4], J. PRAKS[3], (Member, IEEE), M. Z. H. BHUIYAN[1], S. KAASALAINEN[1], AND H. KUUSNIEMI[1,4,5], (Member, IEEE)

[1]Department of Navigation and Positioning, Finnish Geospatial Research Institute (FGI), National Land Survey of Finland (NLS), 02150 Espoo, Finland
[2]Faculty of Information Technology and Communication Sciences, Electrical Engineering Unit, Tampere University, 33720 Tampere, Finland
[3]Department of Radio Science and Engineering, Aalto University, 02150 Espoo, Finland
[4]School of Technology and Innovation, University of Vaasa, 65101 Vaasa, Finland
[5]Digital Economy Research Platform, University of Vaasa, 65101 Vaasa, Finland
[6]School of Marketing and Communication, University of Vaasa, 65101 Vaasa, Finland

Corresponding author: E. S. Lohan (elena-simona.lohan@tuni.fi)

This work was supported in part by the INdoor Navigation from CUBesAT Technology (INCUBATE) Project through the Technology Industries of Finland Centennial Foundation, and in part by the Jane and Aatos Erko Foundation (JAES).

ABSTRACT More and more satellites are populating the sky nowadays in the Low Earth orbits (LEO). Most of the targeted applications are related to broadband and narrowband communications, Earth observation, synthetic aperture radar, and internet-of-Things (IoT) connectivity. In addition to these targeted applications, there is yet-to-be-harnessed potential for LEO and positioning, navigation, and timing (PNT) systems, or what is nowadays referred to as LEO-PNT. No commercial LEO-PNT solutions currently exist and there is no unified research on LEO-PNT concepts. Our survey aims to fill the gaps in knowledge regarding what a LEO-PNT system entails, its technical design steps and challenges, what physical layer parameters are viable solutions, what tools can be used for a LEO-PNT design (e.g., optimisation steps, hardware and software simulators, etc.), the existing models of wireless channels for satellite-to-ground and ground-to-satellite propagation, and the commercial prospects of a future LEO-PNT system. A comprehensive and multidisciplinary survey is provided by a team of authors with complementary expertise in wireless communications, signal processing, navigation and tracking, physics, machine learning, Earth observation, remote sensing, digital economy, and business models.

INDEX TERMS Constellation design, low earth orbit positioning, navigation and timing, LEO business models, receiver optimisation, satellite-to-ground channel models.

I. INTRODUCTION AND MOTIVATION

Investments within the space industry have shifted in the past decade from the Medium Earth Orbit (MEO) satellite-based constellations and applications to Low Earth Orbit (LEO) satellite-based ones. Several LEO systems currently offer a wide range of services, ranging from broadband connectivity (e.g., Iridium, OneWeb, and Starlink) and Internet of Things (IoT) applications (e.g., Hiber, Myriota, etc.) to Earth observation and synthetic aperture radar (EO-SAR) applications (e.g., Iceye, HawkEye, etc.). LEO-based signals have already created a paradigm shift in the field of communication and sensing applications. There is now a worldwide research effort towards a similar paradigm shift in positioning

The associate editor coordinating the review of this manuscript and approving it for publication was Kegen Yu.

applications, i.e., the LEO positioning, navigation, and timing (LEO-PNT) concept [1]–[4].

Traditional satellite-based positioning systems rely on MEO [5] and Geostationary Earth Orbit (GEO) satellite systems, such as the US Navstar GPS (Global Positioning System), the European Galileo, the Russian GLONASS (Globalnaya Navigazionnaya Sputnikovaya Sistema), and the Chinese Beidou, as well as on augmented satellite systems [6], [7] such as the European Geostationary Navigation Overlay Service (EGNOS) in Europe, the GPS-Aided Geo-Augmented Navigation system (GAGAN) in India, or the Wide Area Augmentation System (WAAS)/Canadian WAAS (CWAAS) in the North American continent. Strictly speaking, MEO orbits start at around 2,000 km above sea level and range up to 35,786 km, while GEO orbits are placed at exactly 35,786 km above sea level. However, all satellite-based navigation systems from MEO and GEO nowadays have orbits at least 19,100 km above sea level, which makes their signals reach Earth with a high attenuation due to inherent distance-based path losses during the satellite-to-ground wireless signal propagation.

The first LEO satellites were launched more than 50 years ago and it was only in the 1980*s* that Iridium [8] was launched as a global system for low-latency narrowband communications. Later on, LEO-based broadband constellations, such as OneWeb, Starlink, and Kuiper [9] emerged and aimed to offer high-capacity wireless connectivity globally, especially in remote areas that are hard to access via a terrestrial infrastructure.

In the past few years, LEO potential in the context of positioning and localization has also started to be investigated, and the LEO-PNT concept has emerged. There are three approaches to the use of LEO constellations for positioning:

1) **SoO approach:** LEO signals as signals of opportunity (SoO). No specific positioning signals are transmitted and the burden of the PNT engine is at the receiver end. Measurements such as angle of arrival (AOA), received signal strength (RSS), or Doppler shifts can be used.
2) **Modified-payload approach:** modification of the LEO transmitter payload to support positioning signalling. Global navigation satellite system GNSS) receivers can also be installed onboard the satellites and GNSS-like signals can be rebroadcast in other frequency bands. This can be seen as a ''piggybacking'' solution to LEO signal payloads.
3) **New LEO-PNT approach:** Novel LEO-PNT systems with optimised design parameters for positioning and navigation targets (e.g., [10]).

Our paper addresses several aspects of implementing a LEO-PNT system. The main goal is to find the viable instruments and techniques to be used, possible gains in comparison to classic GNSS, and the overall capability of LEO-PNT systems depending on distinct positioning approaches. Our main contributions are:

- Comprehensive survey of LEO-based positioning systems, methods, and algorithms;
- Unified view of the various signal design considerations;
- Overviewing the parameters of existing and planned LEO constellations;
- Literature review on the various satellite-to-ground and ground-to-satellite channel effects and channel models;
- Presenting state-of-the-art positioning algorithms that can be tailored for LEO-PNT systems;
- Review of the main simulation tools for LEO-based positioning and sensing;
- Perspective on future commercial endeavours in LEO-based services.

Table 1 provides an overview of related surveys in the existing literature and how they compare with the work in our survey. Three manners of addressing a certain topic were identified: i) those who give a full picture of the topic in a self-contained manner; ii) those who partially address a certain topic and are not self-contained; and iii) those who do not address a particular topic but still have relevant material related to other LEO research topics.

As shown in Table 1 our work differs from previous literature by offering a comprehensive view of the three LEO segments (space, ground, and user) as well as of the commercial perspective on LEO-PNT solutions. The next sections comprise first an overview of solutions existing at each of the four segments. Each section ends with a summary of relevant features in the context of the three LEO-PNT approaches (SoO, modified payload, and new LEO-PNT). For the sake of clarity, signal design was treated as a separate section even if it belongs to the space segment.

II. SIGNAL DESIGN CONSIDERATIONS

This section gives a comprehensive overview of the signal design aspects of LEO signals. We discuss the methodology for choosing carrier frequencies and bandwidths and review the possible modulation and channel coding methods. Finally, we address the questions of multiple access (i.e., how different LEO satellites are sharing the wireless channel) and beam forming (i.e., multi-element antenna arrays onboard the satellites and signals sent in directional beams towards the target users).

A. CARRIER FREQUENCY AND BANDWIDTH CHOICES

The frequencies used for satellite communications, navigation, and sensing or Earth-Observation (EO) applications are generally chosen from those that are favourable in terms of power efficiency, minimal propagation distortions and attenuation (e.g., minimal path losses), and reduced noise and interference (e.g., low amount of interference to existing wireless systems sharing the same frequency bands). In addition, the frequency regulations of the International Telecommunication Union's Radiocommunication Bureau (ITU-R) and of individual nations must be obeyed. These conditions force the operation into the frequency regions with best trade-offs. Table 2 shows a summary of the main frequency bands currently used in satellite communications, as well as the

TABLE 1. Related surveys on LEO and the literature, and comparison with our survey.

Reference	LEO Space Segment					LEO Ground Segment		LEO User Segment			Commercial Perspectives
	Signal Design	Constellations	Satellite Communication	Small Satellite Platforms	LEO POD	Architecture	Optimisation	Channel Effects	LEO-PNT Receivers	Positioning Algorithms	
[10]	❍	◗	❍	❍	❍	❍	●	❍	❍	❍	❍
[11]	❍	❍	●	◗	❍	❍	❍	❍	❍	❍	❍
[12]	❍	❍	●	◗	❍	❍	❍	❍	❍	❍	◗
[13]	❍	❍	●	❍	❍	❍	❍	❍	❍	❍	❍
[14]	❍	❍	●	❍	❍	❍	❍	●	❍	❍	❍
[15]	❍	◗	●	❍	❍	❍	❍	●	❍	❍	❍
[16], [17]	❍	●	●	❍	◗	❍	❍	●	●	●	◗
[18]	❍	❍	❍	●	❍	❍	❍	❍	❍	❍	●
[19]	❍	❍	❍	◗	❍	❍	❍	❍	❍	❍	●
[20]	❍	◗	●	●	❍	●	❍	❍	❍	❍	❍
[21]	❍	●	❍	❍	❍	❍	❍	❍	❍	❍	◗
[22]	❍	●	❍	●	❍	❍	❍	❍	❍	❍	●
[23]	❍	❍	❍	❍	❍	❍	❍	❍	❍	❍	●
[24]	❍	●	❍	●	❍	❍	❍	❍	❍	●	❍
[25]	❍	●	●	❍	❍	❍	❍	❍	❍	❍	●
[26]	◗	●	●	❍	❍	❍	❍	❍	❍	❍	❍
[27]	❍	❍	❍	❍	●	❍	❍	❍	❍	❍	❍
[28]	❍	❍	❍	❍	●	❍	❍	❍	❍	❍	❍
Current survey	●	●	●	●	●	●	◗	●	●	●	●

● – topic addressed in detail/self-contained, ◗ – topic partially addressed (i.e., not self contained, requires additional readings for deep understanding), ❍ – topic not addressed

TABLE 2. Frequency bands for satellite constellations with typical usage.

Frequency Band	Frequency	Typical Usage	Constellation Examples	Orbits
UFH	0.3-3 GHz	IoT;	Myriota; Hiber	LEO
L-Band	1-2 GHz	PNT; Communications	GPS; Galileo; Iridium	MEO; LEO
S-Band	2-4 GHz	Communications; Earth observation	Inmarsat; Helios Wire	GEO; LEO
C-Band	4-8 GHz	Communications; Satellite TV	Eutelsat; Telesat	LEO
X-Band	8-12 GHz	Military; Weather monitoring	BlackSky Global	LEO
Ku-Band	12-18 GHz	Communications; TV; Broadband services	OneWeb; StarLink	LEO
K-Band	18-26 GHz	Short-range applications	N/A	N/A
Ka-Band	26.5-40 GHz	TV; Broadband services	Starlink; Kuiper; Teledesic; Viasat	LEO; GEO
Q-Band	33-50 GHz	Communications; Radio astronomy; Gateway links	Jupiter-3; BlueWalker-3	LEO
V-Band	40-75 GHz	Communications; Broadband services	OneWeb; Starlink;	LEO

encountered trade-offs. In addition to LEO satellite orbits, GEO and MEO orbits are also included. Table 2 summarises the IEEE band designation, frequency range, typical usage, examples of constellations that use those frequencies, and the typical orbits (LEO, MEO, or GEO) whose satellite signals are using those frequency bands.

Figure 1 shows the frequency bands listed in Table 2 in terms of the trade-offs in antenna size, spectrum bandwidth, throughput, atmospheric fading, and band usage. There is a clear trade-off between most of these parameters. For instance, maximum theoretical throughput is achieved with higher carrier frequencies due to their ability to support better multiple-antenna-array processing and larger antenna arrays. But then again, the atmospheric attenuation and other path losses are stronger at higher carrier frequencies, and thus the ranges/coverage areas are smaller.

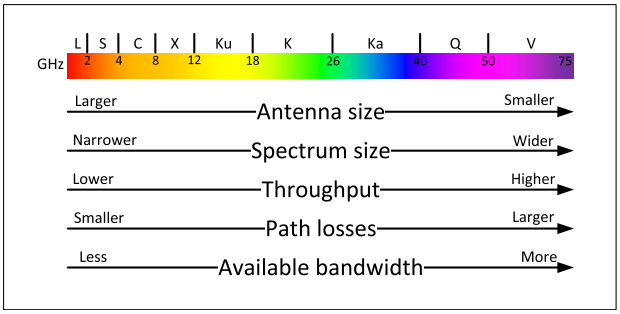

FIGURE 1. Frequency bands with respect to antenna size, spectrum size, throughput, atmospheric fading and usage.

According to Figure 1, there is no clear winner in terms of the frequency band to use in a specific LEO satellite-based application. So the final selection must take into account the regulatory aspects, as well as the cost (e.g., of antenna design). Most LEO systems operate in Ku and Ka bands, and the emerging LEO systems tend to move into higher frequency (Q/V bands). While the carrier frequency of the current LEO systems is mainly used for SoO positioning, new LEO-PNT systems can benefit from carrier frequencies above 5 GHz. Although it may be necessary to keep the

frequency below 12 GHz (C and X bands) to keep path losses at moderate levels, the 5 GHz spectrum would provide less inter-system interference because it is less used.

SoO and modified-payload approaches rely on bandwidths used for communications, widely varying between narrow bandwidths, such as 30 kHz for Blacksky Global, and ultra high bandwidths, such as 100 MHz for Kuiper, 250 MHz for OneWeb, 40 – 400 MHz for Iceye, and 600 MHz for Capella Space.

In code- or code/Doppler-based positioning, the time-based estimation accuracy is known to be proportional to the signal bandwidth. The higher the bandwidth, the more accurate the timing estimation. Therefore, bandwidths of the order of 10 to 100 MHz are recommended. The tradeoff is between the positioning accuracy, the receiver complexity, and the contiguous spectrum availability. If only Doppler-based measurements are used, lower bandwidths are enough to transmit the navigation data. In GNSS systems, bandwidths of up to 1 MHz are recommended. The higher end is suitable for code division multiple access or orthogonal frequency division multiple access, and the lower ends (few tens of kHz) are suitable for time- or frequency- division multiple access.

B. MODULATION CHOICES

The modulation schemes should take into account the purpose of the satellite system, facing a main tradeoff between cost and performance. Throughputs are important in broadband communication. However, in particular to positioning, reliability of the transmissions is more important than maximum achievable throughput, so that high and ultra-high data rates are not needed. For instance, GNSS L1 rate is 50 bits per second and Galileo E1 rate is 250 symbols per second. Hence, low-order modulation methods, along with low-rate channel codes with high error-correction capabilities, are preferable over higher-order modulation schemes with high-rate forward error correction (FEC) codes [26]. When a LEO system has the dual purpose of communication and positioning, the criteria for the best modulation and coding should include both positioning and communication metrics (e.g., reliability, throughput, spectral and energy efficiency).

The vast majority of the available or planned LEO systems rely on digital modulations. For this reason, we overview the available digital modulations and do not focus on analog ones. Tables 3 and 4 list the main available modulation techniques for LEO signals, grouped into linear (Table 3) and non-linear modulation (Table 4), respectively. Advantages and disadvantages are discussed for each modulation family, and examples of LEO constellations employing some modulations are also given. In some cases, the same system (e.g., Starlink, Oneweb) appears as an example under several modulation types; this means that a certain system can use more than one modulation type.

In linear-modulation techniques, such as those listed in Table 3, the principle of superposition applies, meaning that linear superposition of inputs is seen as linear superposition of outputs; also, if the input is scaled by a certain factor, the output of the modulator is scaled by exactly the same factor. Non-linear modulation techniques do not fulfil this superposition principle. They usually have a lower spectral efficiency than linear modulation techniques, but they may have a slightly better robustness to Doppler error.

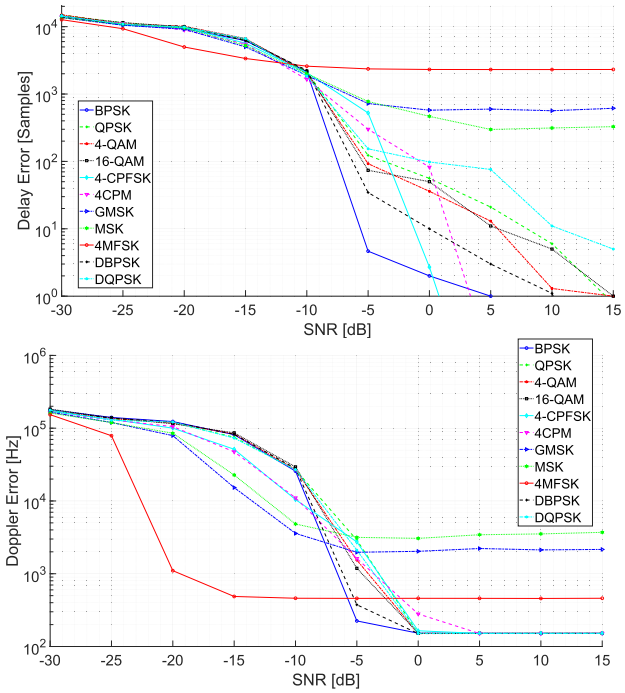

FIGURE 2. Performance of various modulations considering time and frequency measurements.

Most LEO constellations use low-order linear BPSK or QPSK modulations (e.g., Globalstar Iridium Next, OneWeb, RapidEye). A few medium and small-sized constellations also use nonlinear low order modulations, such as GMSK (e.g., Myriota). A few mega-constellations aiming at ultra broadband communications have opted for high-order modulations, such as M-QAM with M up to 64 in Starlink and 64-APSK for Telesat.

Figure 2 shows the performance of 11 different linear and non-linear modulations listed in Table 3 and Table 4 in a scenario with multipath. We clearly observe that any of the considered modulation performs equally well with both time and frequency measurements. Phase (e.g., BPSK, QPSK, or CPM) modulations typically behave better measuring the delay, while frequency modulations (e.g., MFSK, GMSK) typically behave better with frequent measurements. Although the low-order BPSK/QPSK or GMSK modulations seem more appropriate for LEO-PNT, the BPSK modulation is more suitable for time-based positioning due to its linearity and simplicity, while GMSK is more suitable for Doppler-based positioning as it is more robust to Doppler errors.

C. CHANNEL-CODING CHOICES

Channel coding is employed to protect wireless signals against channel errors. It relies on redundancies added to the signal, and therefore it increases the transmitted symbol

TABLE 3. Summary of linear modulation techniques and their applicability to LEO signals.

	Modulation Type	Advantages	Disadvantages	Description and Examples	Ref.
Linear	M-ary Amplitude Shift Keying (M-ASK) and On-Off Keying (OOK)	High bandwidth efficiency. Simple receiver design and inexpensive.	Rather inefficient and susceptible to channel interferences (noise affects the amplitude). Non-constant envelope; it needs highly linear power amplifiers.	Binary ASK is also called OOK. This modulation changes the amplitude of the carrier according to the signal to be transmitted. Currently not in use for LEO signals.	[29]–[31]
	M-ary Phase Shift Keying (M-PSK) (e.g., BPSK, QPSK, etc.)	Efficiency is high and it is less susceptible to channel errors compared to M-FSK and M-ASK.	Side lobes interfere with adjacent carriers.	This modulation changes the phase of the analog carrier to transmit the data. Examples: Starlink uplink (BPSK), OneWeb (QPSK, 8-PSK), Hawkeye (BPSK, QPSK).	[32]
	M-ary Amplitude and Phase-Shift Keying (M-APSK)	Low peak-to-average power ratio (PAPR). Better spectral efficiency than M-PSK and better resistance to channel distortions than M-QAM.	Modulation/demodulation has higher complexity than stand-alone M-ASK/M-PSK, and it requires optimisation.	It is a generalisation of M-ASK and M-PSK, and it can be considered as a superclass of M-QAM, as it includes M-QAM cases, plus cases where all symbols are either all real or all imaginary. Examples: Planet Labs (16-APSK), Telesat (64-APSK), Oneweb (256-APSK), Viasat (32- and 64-APSK).	[32]–[34]
	M-ary Quadrature Amplitude Modulation (M-QAM)	Better data-carrying capacity than M-ASK and M-PSK. Supports high data rates. High spectral efficiency and low symbol distortion.	It is susceptible to noise (especially for high-order modulations).	Higher M means higher spectral efficiency. Examples: Starlink, OneWeb (16-QAM).	[32]

TABLE 4. Summary of nonlinear modulation techniques and their applicability to LEO signals.

	Modulation Type	Advantages	Disadvantages	Description	Ref.
Non-linear	Symmetry chirp spread spectrum (SCS)	Reduces the cross-correlation level caused by Doppler shifts. Smaller cross-correlation than chirp spread spectrum (CSS) with similar autocorrelation gain.	Lower performance than CSS in terms of interference.	The waveform is divided into subsections and a different (but symmetric with respect to the bandwidth) chirp rate is applied to each subsection.	[35], [36]
	Asymmetry chirp signal (ACS)	Keeps good auto-correlation compared with SCS and has better cross-relation than SCS in time and frequency domains.	Varying the effective wavelength λ_{eff} may increase the positioning accuracy.	It is a type of revised SCS in which the λ_{eff} is varying (in contrast with SCS, which has constant λ_{eff}).	[37]
	Chirp Spread Spectrum (CSS)	Can be used both as modulation and multiple access scheme.	CSS modulation cannot be directly applied to satellite constellations due to large cross-correlation.	Data between different users is distinguished by using different values for the start frequency of chirp signals.	[37], [38]
	Differential encoded QPSK (DEQPSK)	More robust to Doppler effects than QPSK; can remove the phase ambiguities specific to QPSK.	Complex Tx/Rx.	It employs a single-stage differential modulation. Example: Iridium.	[39]
	Double differential MPSK (DDMPSK)	Robust to Doppler effects.	Complexity of the Tx/Rx.	It employs a two-stage differential modulation by which the Doppler effect due to satellite orbiting motion is nullified.	[40]
	Frequency shift keying (FSK)	FSK Tx and Rx implementations are simple. Less susceptible to errors and interference than ASK because interference is often confined to a specific frequency.	Bandwidth efficiency is not as high as with ASK.	It shifts the frequency of the carrier to modulate the data.	[41]
	Gaussian filtered minimum shift keying (GMSK)	There are no phase discontinuities. Side lobes in the spectral density are low, which produces less interference and uses the spectrum better. Excellent power efficiency due to a constant envelope.	Main lobe is narrower than using MSK modulation. Filtering can cause inter-symbol interference. A higher power level than QPSK.	It is a modified minimum shift keying (MSK) modulation where the phase is filtered through a Gaussian filter to smooth the transitions from one point to the next in the constellation. This decreases the side lobes power. Example: Myriota.	[42]

rate; in other words, the spectral efficiency decreases. Consequently, higher-order channel codes are more wasteful of bandwidth resources, while offering better protection against channel errors compared to lower-order channel codes. Table 5 lists the main available channel-coding techniques, compares them in terms of advantages and disadvantages, and lists some examples used in current and planned LEO systems.

A numerical comparison of four main channel coding techniques, namely convolutional, Turbo, LDPC, and polar codes

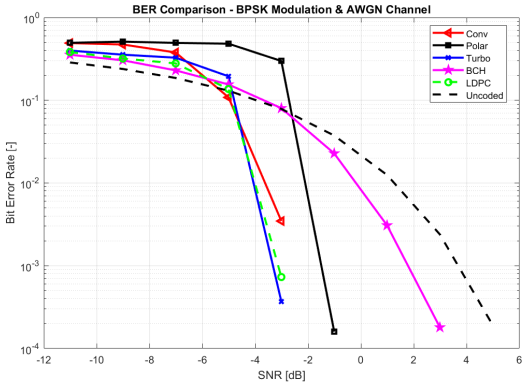

FIGURE 3. Comparison of various channel-coding techniques for a BPSK-modulated signal.

was provided in [47] with BPSK modulations. It was shown that the best performance at low signal-to-noise ratios is achieved with simple convolutional codes, while Turbo coding gives the best performance at moderate and high signal-to-noise ratios. Following the approach in [47], we have also selected five channel-coding types from Table 5, and compared them in Fig. 3 for a BPSK-modulated signal of 20 MHz bandwidth and 10 GHz carrier frequency. The uncoded bit error rate is also shown as a benchmark. The best performance is achieved with Turbo, convolutional, and LDPC channel coding. The convolutional coding offers the lowest decoding delay and lowest complexity among the three, followed by Turbo coding.

Based on Table 5, the numerical analysis from [47], and our numerical results, convolutional coding seems more suitable for LEO-PNT systems targeting low complexity and delay-sensitive receivers. On the other hand, turbo coding is advisable for high-grade delays-tolerant receivers.

D. MULTIPLE-ACCESS CHOICES

Three types of measurements can be used for positioning purposes: Doppler, pseudorange, and carrier phase. If the carrier phase is used, the signal must be continuous [48]. For this reason, multiple access methodologies such as time division multiple access (TDMA) are not applicable for satellite positioning because transmissions are split into different time slots and the transmissions are not continuous.

If the transmitted signal is continuous, a delay lock loop (DLL) and a frequency lock loop (FLL) can be used to obtain the pseudorange and Doppler-shift measurements, respectively [49]. On the contrary, if the signal is not continuous, open loop estimation techniques must be used. Neither space division multiple access (SDMA) nor polarisation division multiple access (PDMA) are applicable because a receiver should get transmissions from at least four satellites to calculate the 3D position. SDMA by itself cannot provide more than a single satellite or, otherwise the signal transmissions would interfere with each other. PDMA is only able to provide two satellite transmissions at a time using two different polarizations (i.e., horizontal and vertical). Therefore, the only options are frequency division multiple access (FDMA), code division multiple access (CDMA), and orthogonal frequency division multiple access (OFDMA).

FDMA and OFDMA are more sensitive to Doppler shifts, which, combined with the fact that LEO constellations suffer more Doppler shifts than those at higher altitudes, makes FDMA and OFDMA not advisable if positioning is based on Doppler/frequency measurements.

E. BEAMFORMING ASPECTS

Beamforming via LEO satellites is typically needed to increase the satellite footprint or Earth coverage area. In order to serve as many users/devices on Earth as possible with sufficient quality of service, multiple input, multiple output (MIMO) approaches have been proposed to be used both onboard LEO satellites and on user devices [50], [51]. Various antenna array structures have been proposed, such as interlaced triangular lattice antenna arrays [52] or multi-beam phased arrays [53], [54]. The current general understanding is that a large number of beams will be supported at the satellite side, the ground station side, or both. This enables beam-based multiplexing and possibly beam-based positioning, a concept not yet investigated, but listed as a potential future research direction in [55].

F. SUMMARY OF SIGNAL-DESIGN CONSIDERATIONS

We contemplate four main topics for signal design consideration: modulation, channel coding, multiple access scheme, and beamforming. The outcome is that the modulation scheme of a dedicated LEO-PNT system will not need to support high rates of data. For this reason, low-order modulations are the most promising for PNT purposes, but so far there is no clear preference for linear or non-linear ones. Non-linear modulations are more robust to Doppler shifts, but additional research is needed to fully understand the trade-offs between modulation complexity of implementation and its robustness to various channel impairments. The same applies to channel coding. The chosen channel coding scheme will need to achieve an acceptable trade-off between computational and spectral efficiency, where low-complexity channel coding solutions (e.g. convolutional coding) will most likely be enough for reaching LEO-PNT targets. The most likely candidates for multiple access schemes are CDMA and OFDMA, although further analysis is needed to be able to choose among them. The sensitivity of OFDMA with respect to Doppler shifts is a critical aspect and one that may make CDMA techniques more suitable than OFDMA techniques for dedicated LEO-PNT system. Finally, the future PNT-system can benefit from the latest advances in MIMO, increasing even further the performance of the system and enabling novel positioning solutions such as fingerprinting based on beam patterns.

Table 6 summarises the signal design considerations when comparing distinct positioning approaches. The most flexible, but also the most costly, is the new LEO-PNT approach, designed from scratch only with navigation targets in mind. The most rigid, but the least expensive, is the SoO approach,

TABLE 5. Main coding techniques and their suitability for LEO signals.

Coding Technique	Advantages	Disadvantages	Description and examples	Ref.
Block codes	It is the easiest and simplest technique to detect and correct errors. Error probability is reduced.	The information cannot be extracted until the whole code is received. The entire block must be retr smitted in the case of an error. Transmission bandwidth requirement is high, and extra bits reduces bit rate.	Coding and redundancy are implemented at block level. Memory-less between consecutive blocks. Both hard and soft decoding are possible on the receiver side.	[43]
Cyclic redundancy check (CRC)	Very efficient decoding methods due to very rich algebraic structure.	Are meant for simple error detection, not for error correction.	A type of block code in which any arbitrary cyclic shift of any valid code word yields another valid code word. Some examples of CRC codes are Reed-Solomon (RS), and Bose-Chaudhuri-Hocquenghem (BCH).	[44]
Convolutional codes	Better performance than block codes. Best for very large data streams. More energy efficient than block codes when you have large streams of data	Computational complexity increases exponentially with the length of the code.	Coding also done at block level, but with memory between consecutive blocks. Both hard and soft decoding are possible on receiver side, although Viterbi soft decoding is typically used.	[43]
Fountain codes	Performance close to Shannon limit.	Not need to know the rate of packet loss.	Rateless codes that allow recovery of the original message through the reception of any subset of the packets (or "drops"), as long as the number of packets received is higher than the size of the original message.	[45]
Low-density parity check (LDPC)	Efficient iterative decoding with reasonable complexity. Performance close to capacity.	The encoding complexity is higher than for turbo codes. Iterative LDPC decoding typically requires many more iterations than iterative turbo decoding, which may lead to a higher latency.	Special case of block codes with sparse structure for parity check. Examples: Amazon Kuiper.	[43], [46]
Polar codes	Maximum performance is equal to capacity.	The coding is optimized for a specific SNR. Operating at different SNR points requires different code designs	Special case of block codes with capacity-achieving properties. They are based on the channel polarization phenomenon.	[43]
Trellis codes	The data rate can be increased without increasing the bandwidth by transmitting more information per symbol. The information content of the symbol is increased by increasing the number of possible symbol values.	For high spectral efficiencies a high-rate convolutional code is required. Bigger noise sensitivity in the large symbol alphabet	A combination of coding and modulation in which the idea is to build redundancy such that symbol alphabet design depends on the code rate. Soft decoding is typically deployed.	[43]
Turbo codes	Performance close to Shannon limit.	High latency due to interleaving and iterative decoding. High decoding complexity.	Two or more interleaved convolutional codes, commonly in parallel. An interleaver allows for efficient iterative decoding at RX.	[43]

where existing LEO signals is used without any dedicated design at the transmitter side. The middle-ground solution is the modified-payload approach, where the navigation payload is added on-board of LEO satellites with some parameters, such as the multiple access and beamforming, dictated or limited by the initial design of the satellites.

III. SPACE SEGMENT

The space segment is composed of a constellation of satellites transmitting RF signals to users. The main elements of interest to materialise the space segment are the satellite platform, onboard instruments, and constellation design. This section provides details about these elements, including viable options of instruments and techniques to be considered in the upcoming LEO-PNT systems. Additionally, orbit optimisation and cost estimation are discussed with particular interest to the navigation systems.

A. PLATFORM AND ONBOARD INSTRUMENTS

In the following subsections, we present considerations about the satellite platform and the navigation payload. To analyse

TABLE 6. Recommended choices for three alternatives of a LEO-PNT. Some (e.g., new LEO-PNT) have much more flexibility than others in setting the signal parameters.

	SoO	Modified Payload	New LEO-PNT
Carrier Frequency	defined by the SoO system; most usual in Ka/Ku band, see Table 2	defined by the LEO system where navigation payload is added; most usual in Ka/Ku band	$5-12$ GHz as a tradeoff between low interference with existing systems and low path losses
Bandwidth	defined by the SoO system; most usually above 100 MHz to support communication needs	defined by the LEO system where navigation payload is added; navigation payload may need a smaller bandwidth than its communication counterpart	maximum 1 MHz is enough for systems relying on Doppler-based positioning; $10-100$ MHz recommended for systems relying on code- or code/Doppler-based positioning.
Modulation	defined by the SoO system; most common modulations are PSK and MSK	can be defined by the LEO system where navigation payload is added or can use a simple modulation (e.g., BPSK) for the navigation payload	determined by minimising the non-desired effects for positioning
Channel coding	defined by the SoO system; most common channel-coding schemes in use are the convolutional codes	can be defined by the LEO system where navigation payload is added, same as for a SoO, or can use a simple channel coding for low complexity (e.g., convolutional coding) for the navigation payload	convolutional coding for low-complexity delay-sensitive receivers and Turbo coding for high-grade delays-tolerant receivers.
Multiple access	defined by the SoO system; most common multiple-access schemes in existing LEO systems are low-order modulations, such as BPSK, QPSK, and GMSK	mainly defined by the LEO system where navigation payload is added. it might differ with respect the original SoO system with some limitations	determined by the LEO-PNT system configuration. The only limitation is the compatibility and/or hardware
Beamforming	defined by the SoO system	defined by the LEO system where navigation payload is added, same as for a SoO	no beamforming or transmitter with large main-beam antennas for wide coverage on Earth

the navigation payload, we selected onboard antenna and clocks since they have the strongest impact on the cost and accuracy of a LEO-PNT system.

1) PLATFORM CONSIDERATIONS

Satellite platforms are the structures in which the payload and all scientific instruments are mounted. Basic subsystems of a small satellite platform include command and data handling (CDH), attitude and orbit control system (AOCS), electric power system (EPS), thermal control system (TCS), mechanical structure (STR), and telemetry, tracking, and command (TTC) [56], [57]. These subsystems are briefly described in [18], [20], [56], [58]–[60] and [61].

The efficiency and quality of the subsystems mainly depend on the weight the platform can carry. Despite heavier platforms have great benefits, they usually require dedicated launches for injecting the satellite's mass into the required orbit. These dedicated launches slow down the whole mission implementation and, foremost, increases considerably the total cost of the mission. Dedicated launches can cost over €10 million Euros. On the other hand, smaller satellites can be carried as a secondary payload, providing significant cost reduction. According to the metrics provided by [62] at the moment this work is conducted, the launch of microsat platforms with 6U is about €300,000, being 1U equals to $10 \times 10 \times 10$ cm. To demonstrate the importance of the launch, and indirectly the platform mass, to the total cost of a satellite mission, [62] shows a rough approximation of $\textit{total cost} = 3.5(\textit{launch cost})$.

As demonstrated later in this section, dedicated LEO-PNT systems will require the materialisation of hundreds of satellites. In this scenario, small satellites seems to be the most feasible option for dedicated systems. We therefore present Table 7 as the main possible options of platforms in upcoming LEO-PNT systems. A major drawback of these small satellite platforms, however, is the power consumption. There are intrinsic limitations in the small satellites since they cannot support high consumption power requirements. Hence, dedicated studies are necessary to define the best platform given the power consumption requirements of the payload. Onboard clocks and antenna can be considered as the main equipment to increase the payload size and power consumption. The next subsections, therefore, present a discussion of possible clock and antenna options for LEO-PNT systems.

2) ANTENNA DESIGN

The satellite antenna is highly influenced by the following criteria [63]: the frequency band used during the transmissions (L-band, C-band, Ku-band, etc.), the maximum radiated power, power consumption, the size of the satellite, and the desired coverage per satellite. Classical GNSS systems based on MEO satellite use patch and quadrifilar helix antennas. However, this may not be an option for the upcoming LEO satellites. To indicate a few possible options, we present the most frequently used antenna types for space applications in LEO heights.

- **Wire Antennas** comprise monopoles, dipoles, helical antennas, and Yagi–Uda arrays [63]. These antennas are kept folded and are deployed after launching, since they are typically placed externally. Wire antennas are especially common for high frequency (HF), very HF (VHF), and ultra HF (UHF) applications, where the wavelength is longer. These antennas are easy to build and provide good radiation efficiency within a relatively small volume at a contained price.
- **Reflector Antennas** offer high gain, high directivity, and good resolution, but they come with increased mechanical complexity. These antennas are external and deployed after launching. Reflector antennas are typically used with C-, X-, Ku-, and Ka/K-bands [11], [63]. Moreover, they can be used in multi-band and multi-beam applications. The main drawbacks of these antennas are that are typically bulky (especially at low frequency) and heavy, which make difficult to integrate in small-sized satellites [11]. To partially solve this issue, inflatable reflector antennas were proposed by the authors in [64]. These antennas are folded during launch and deployed after reaching orbit.
- **Reflectarray Antenna** is a planar array of reflective elements illuminated by a feed [65]. Since their structure is flat, they can be easily integrated in small satellites. These antenna types, given their contained size, are typically used for high frequency band applications (e.g., C-band and above).

TABLE 7. Small satellite platforms [59], [61].

Small Satellites	Mass [kg]
Cubesat	$\leq$ 1.33 kg per U
Picosat	$\leq$ 1
Nanosat	1 – 10
Microsat	11 – 100
Minisat	101 – 500

- **Membrane Antennas** are thin, fabric-based antennas, which can fold during launch and can fit into small satellites [66]. Membrane antennas are typically used for frequencies ranging from UHF to K-band [67].
- **Horn Antenna** is a rectangular or, more commonly, circular piece of a waveguide [68], broader at the open end. Horn antennas are especially useful at high frequency bands, from K-band onwards [66], but can also be used at lower frequency bands.
- **Patch Antennas** are one of the most used antennas because they are easy to fabricate, have a low profile and low cost, and are easy to integrate [69]. Patch antennas are typically used in S- C- and X-bands, providing a typical gain ranging from 4.8 to 30.5 dBi [11].

3) CLOCK ON BOARD

Space-based navigation systems rely on stable atomic clocks to define a space-time reference frame. They serve applications worldwide since space systems allow the synchronisation of electronic devices in the ground over large regions. A major challenge is the need for stable and continuous frequencies. In the case of GNSS, if the clock time is not sufficiently stable, or if its frequency drifts are unpredictable, the pseudoranges accumulate significant errors. Assuming that a 1 m precision is needed in the pseudorange measurements, 3 ns timing uncertainty is required for signals travelling at the speed of light. Maintaining 3 ns timing uncertainty for one day requires a frequency stability of [3ns/86400s]=3.5×10^{-14}, which is achievable with atomic clocks but not with other kinds of clocks [16]. A detailed analysis of several clock performances is provided by [70].

MEO satellite-based navigation clocks are made by passive hydrogen maser and rubidium atomic frequency standards, which rely upon lamps and magnetic state selectors. Considerable research has shown the benefits of replacing discharge lamps for optical pumping and laser-driving systems; however, these state-of-the-art clocks remain on the ground [16]. Alternative proposals have been made to use more stable atomic clocks in future space missions. As shown by [71], two-way lasers, or microwave links, could be used to synchronise highly stable clocks in space. Indeed, lasers have higher spectral purity and brightness than lamps, and enable atomic clocks with better stability and accuracy, but at the expense of complexity, reliability, and cost. Additionally, optical atomic clocks can achieve better stability and accuracy, but they are much more complex and are not currently robust enough for navigation systems. The future optical atomic clocks are likely to find their way into space navigation missions.

The atomic clocks used nowadays as references for PNT applications are too large and consume too much power for use in small LEO payloads. To overcome this issue, recent advances in Photonics and microelectromechanical systems (MEMS) have shown the possibility of creating low-power and small-volume atomic clocks. Zhang *et al.* [72], for instance, developed a low-power, miniaturized atomic clock system with a cesium gas cell by using laser and advanced complementary metal-oxide semiconductor (CMOS) circuits. The prototype achieved a long-term Allan deviation of 2.2×10^{-12} (10^5s) stability and a short-term Allan deviation below 8.4×10^{-11} (1s) stability.

Another solution to the high volume and power consumption of stable atomic clocks is to adapt heterogeneous clock systems and exploit the reference time from a GNSS receiver onboard a LEO satellite. In this regard, Van Buren *et al.* [73] designed an architecture that uses a single-crystal oscillator, one or more chip scale atomic clocks (CSACs), and a space-borne GPS receiver. This heterogeneous group of oscillators is combined in order to discipline the crystal oscillator and obtain overall system stability for timeframes ranging from less than a second to several days.

In addition to the natural presence of noises and instabilities, clocks in orbit experience relativistic frequency shifts. The relativistic effects need to be considered since the frequency of a clock tick on a satellite differ from those of a clock on the ground, mainly because satellite clocks are moving much faster than clocks on the ground, and they experience a much lower gravitational force. A formulation often used to consider the relativity in precise GNSS positioning is:

$$\tau = -2(\mathbf{r} \cdot \mathbf{v})/c^2 \tag{1}$$

where $\mathbf{r}$ and $\mathbf{v}$ are the satellite position and velocity vectors, respectively. As discussed by [74], the approximations conducted to derive equation (1) are nearly negligible at the altitude of a GNSS satellite orbit; however, a more appropriate formulation can provide markedly better results at the LEO satellite altitudes. The numerical integrations proposed in [74] better consider the Earth's gravitational potential. Despite the heavier implementation requirements, the numerical integration of the periodic relativistic effects may take the place of equation (1) in LEO-PNT navigation systems.

B. CONSTELLATION DESIGN

Constellations are composed of multiple satellites deployed in various orbital planes to accomplish the requisite coverage for a common application. The orbital planes within the constellation are separated by the right ascension angles relative to a reference plane, and are deployed based on orbital parameters. The orbital parameters include altitude, inclination, eccentricity, number of orbital planes, and number of satellites per plane. Figure 4 highlights the principal parameters for a constellation design.

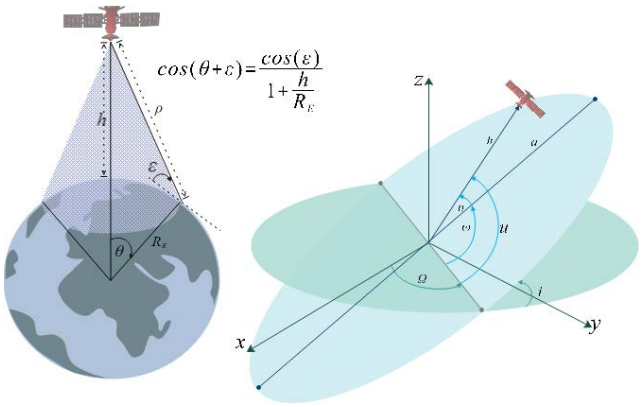

FIGURE 4. Coverage geometry and orbital parameters: ϵ is the elevation angle of the viewing cone of the satellite, h is the satellite altitude, R_E is the Earth's radius, and θ is the central angle of coverage. Semi-major axis a, eccentricity e, inclination i, argument of perigee ω, right ascension of the ascending node (RAAN) Ω, and mean anomaly M are the orbital parameters [75], [76].

To define the best design for a specific application, the orbital parameters need to be optimised accordingly to the mission requirements. In dedicated LEO-PNT systems, the constellation design keeping a continuous 4-fold with global coverage (minimum of 4 satellites in view at any time and location) is the main requirement. The minimum number of satellites required for a 4-fold global coverage can be found as [75]:

$$N_{minsv} = \frac{4K}{1-\cos(\theta)} \tag{2}$$

where $K = 1, 2, \ldots$ is the k-th fold coverage desired in the constellation ($K = 4$ in our analysis).

The minimum number of orbital planes to achieve global coverage is computed as [77], [78]:

$$N_{minPlane} = \frac{360}{2\theta} \tag{3}$$

where θ corresponds to the cap angle (in degrees).

Finally, the minimum orbit inclination to satisfy full global coverage can be computed as [79]:

$$i_{min} = \max(\Phi_{max} - \theta, 0), \tag{4}$$

where i_{min} is the minimum inclination angle (in degrees), Φ_{max} is defined as $max(|\phi_l|, \phi_u)$, with ϕ_l and ϕ_u being the minimum and maximum latitudes comprising the desired coverage area, respectively.

Figure 5 shows simulations of the minimum number of satellites to achieve 4-fold coverage, as well as the minimum number of orbital planes and orbit inclination to achieve global coverage. Assuming an orbit altitude of 600 km, for instance, we can extract from Figure 5 that the minimum required number of satellites is 400, the minimum number of orbital planes is 10, and the minimum inclination is 75°. We can observe that the number of satellites and planes decreases as the altitude increase, i.e., higher altitudes provide better coverage. Nevertheless, the distribution shows an asymptotic pattern, in which no relevant improvements

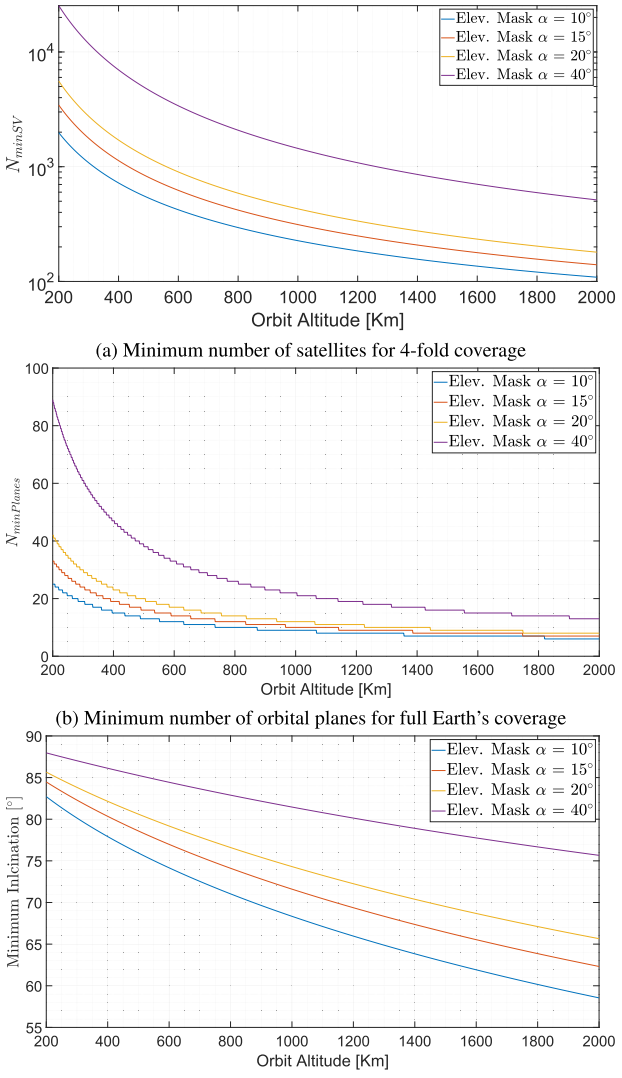

(a) Minimum number of satellites for 4-fold coverage

(b) Minimum number of orbital planes for full Earth's coverage

(c) Minimum orbit inclination for full Earth's coverage

FIGURE 5. Minimum number of satellites in orbit for 4-fold coverage, minimum number of orbital planes, and minimum inclination for full global coverage as a function of orbit altitude.

in the number of satellites and planes are obtained above 1000 km. Therefore, altitudes around 500-1000 km are reasonable regions to deploy the LEO satellite, which also keep a reasonable balance between path losses and drag forces due to the Earth's attraction, as shown in Figure 6.

In addition to the orbital parameters, the constellation design also comprises a topology selection with the primary objective to maximise efficiency while minimising overall system costs [80]. Figure 7 shows visual examples of constellations with distinct topology and at different altitudes, inclinations, and number of orbital planes. The Walker delta is usually the preferred topology by GNSS systems since they keep a symmetric coverage by the user in the ground. However, other options do exist, as presented in the following ([81] and [75]):

- **Street of Coverage**: Street-of-coverage (SoC) constellations consist of satellites in orbital planes with the same altitude and inclination. The coverage is determined by

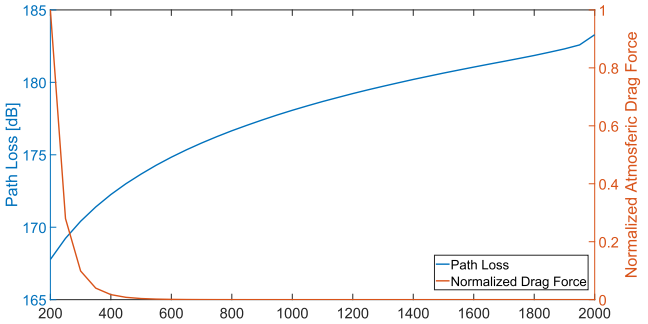

FIGURE 6. Typical path loss and drag force experienced by a satellite orbiting at different altitudes. Transmitted effective isotropic radiated power is set to 69dBm.

the number of satellites, the phase distribution within the plane, and the plane separations. The distribution of orbital planes in SoC is nonsymmetric [75], [76].

- **Draim Constellation**: Draim constellations employ elliptical orbital planes with the same period and inclination. In this configuration, a broad range of orbital parameters can be used, providing wider constellation design options. Compared to constellations with circular or near-circular orbits, elliptical orbits require fewer satellites for coverage.
- **Flower Constellation**: Flower constellations are defined in a rotating frame of reference [82]. Most flower configurations are symmetric, with satellites having the same semi-major axis, eccentricity, inclination, and argument of perigee. The distribution in orbits is acquired through variations in mean anomaly and RAAN. Flower constellation configurations exist in 2D [83] and 3D lattice flower [84] and in 2D and 3D necklace flower [85], [86]. Flower constellations are more complicated to implement, but provide better coverage.

Despite many LEO constellations use the Walker pattern, geodetic positioning is a secondary application in the current LEO constellations. Today's LEO constellations are mainly used as SoO, hence there are no navigation requirements to the constellation design. A few options of already developed constellations typically used in SoO positioning are shown in Table 8. These LEO constellations, including Globalstar, Orbcomm, Iridium, and Iridium NEXT, were first developed for communications; however, as shown later in Section VI, they have found great applicability in SoO positioning.

C. SUMMARY OF SPACE SEGMENT CONSIDERATIONS

We have discussed aspects such as antenna type, clock on board, and available satellite platforms. In this regard, the most likely antenna type to be used will be influenced by the operating carrier frequency. For low or relatively low carrier frequencies (e.g., VHF, UHF, L-band, S-band), larger antenna types will be needed. Antenna types in these bands are typically wire, patch, and slot antennas. On the contrary, at higher frequency bands (e.g., Ku-band, K/Ka-band) reflectors and reflect-arrays antennas are typically used. Since antenna sizes

TABLE 8. Fully-deployed LEO Constellations with Global Coverage [25], [58], [88]–[91].

Name	# N_P	# Sat	i [deg]	h [km]	m_{sat} [kg]	Services
Globalstar	8	48	45	1414	700	Voice, Data
Orbcomm	4	50	45	825	172	IoT, M2M
Iridium	6	66	86.5	780	689	Voice, Data
Iridium NEXT	6	66	87	780	860	Voice, Data

and weights rather vary, dedicated studies are required to define the proper platform type depending on the wanted carrier frequency.

As for satellite clocks, instrument size and power consumption by highly stable atomic clocks are the biggest challenges. Recent advances show the possibility of creating miniaturized atomic clock systems with a cesium gas cell and advanced CMOS circuits. Another prominent solution guides us in the direction of exploiting the time reference of GNSS receivers onboard a LEO satellite. In this way, it is possible to synchronise a heterogeneous group of oscillators and obtain overall clock stability. Despite these efforts, state-of-the-art optical pumping and laser-driving clock systems are still on the ground, so that atomic clocks using lamps and magnetic state selectors are still the only ones used for time reference in PNT applications. The relativistic effects on the clocks also need special attention since the formulations used today for GNSS positioning require non-negligible approximations. In this regard, we observed in the literature that numerical integration considering Earth's gravitational potential provides remarkable improvements for the altitudes of LEO satellites.

Regarding the constellation design, our investigation has shown that Walker delta seems to be the most straightforward choice for the constellation topology, despite other options do exist. In addition, we have observed that several options of constellation parameters can be adopted to optimise a dedicated LEO-PNT system. Table 9 summarises the constellation parameters computed based on our simulations. We mainly highlight the results obtained for the dedicated LEO-PNT systems, which needs to keep a continuous 4-fold with global coverage. From Table 9, we notice that around 400 satellites are necessary for new LEO-PNT systems. With this number of satellites on mind, and knowing that the total mission cost is equal to 3.5 times the launch cost for a six-year lifetime, we can conclude that €1 billion is a realistic mission cost to implement a dedicated LEO-PNT system, which is a significant reduction when compared to MEO-PNT systems. Galileo, for instance, had an estimated cost of €10 billion.

IV. GROUND SEGMENT

The ground segment deals with the maintenance tasks of the satellite system. It involves ground-stations to perform the precise orbit determination, ephemeris computation, clock corrections estimation, and periodic updates of the satellite messages and other parameters. This section discusses the

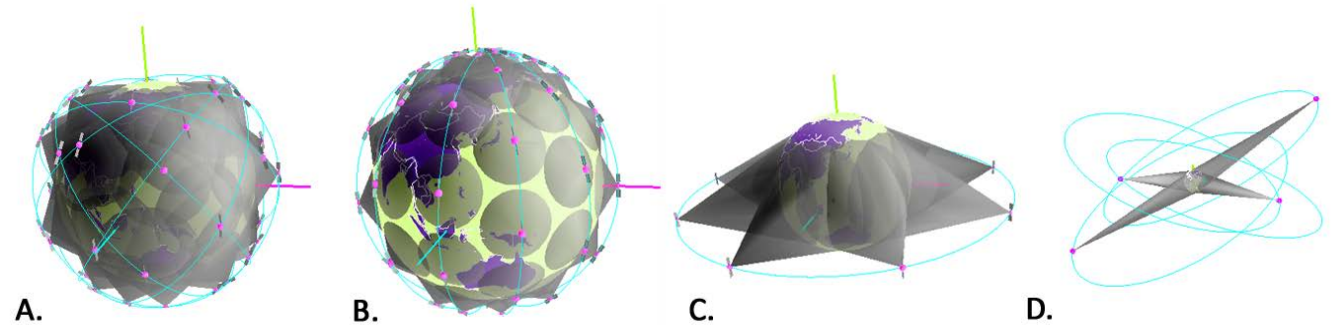

FIGURE 7. Visualization of constellations created with *SaVi* [87]: *A.* Walker constellation with 8 orbital planes and 6 satellites per plane at a 53-degree inclination. *B.* Walker star constellation with 6 polar orbital planes having 11 satellites per plane. *C.* MEO Constellation satellites distributed evenly in the orbital plane *D.* Draim constellation of 4 satellites.

main aspects of the ground segment that may differ from those in classical GNSS.

A. GROUND STATIONS OPTIMISATION

The ground segment is composed by ground stations strategically located worldwide to track, monitor, and communicate with the satellite system. Unlike MEO or GEO systems, LEO orbit and clock determinations can be made independently of ground stations since LEO satellites can carry spaceborne GNSS receivers. However, few studies focus on optimisation of the LEO ground segment. The ground stations optimisation primarily deals with the determination of the optimal number and placement of ground stations to obtain the best performance at monitoring, management, and control of satellites. Since this issue is not specific to LEO satellite systems from an optimisation point of view, we review studies based on MEO and GEO satellite systems.

Some of the most common metrics and techniques for obtaining the best location for a ground station are summarised in Table 10. The example studies share similarities in their metrics and evaluations. As main metrics the optimisation, [92] considers signal availability level, number of visible satellites, geometric dilution of precision (GDOP), scintillation fade depth, ionospheric delay, and rainfall attenuation. In case of [93], ground station network optimisation is studied with particular interest in the effect of rain attenuation on system availability. The key factors identified in the optimisation problem include satellite availability, ground station switching strategies and the number of ground stations on the network. Additionally, the work in [94] has defined the 'quadruple coverage' as the main metric, i.e., at least four ground stations are observed by the same satellite.

Due to the inherent gains of LEO satellites, metrics that depend on the geometry and signal-to-noise ratios may become the primary options for ground stations optimisation in LEO-PNT systems. The approaches proposed by [49], [95], and [92] are highlighted here due to the GDOP and satellite visibility dependency. Other common metrics, such as cost estimations, coverage, and atmospheric delays, are also often discussed, but they rarely share common models in different studies, and are therefore not considered as options.

TABLE 9. Orbital altitude, total number of planes, total number of satellites and orbit altitude to keep requirements of LEO-PNT systems.

	SoO	Modified Payload	New LEO-PNT
Orbit altitude	Is determined by non-navigation requirements whose transmissions are used as SoO.	Is determined by by a mix between non-navigation and navigation requirements.	500-1000km
Number of satellites			around 400
Number of orbital planes			$\geq$10
Orbit inclination			>75°

B. PRECISE ORBIT DETERMINATION

The traditional satellite orbit determination for LEO is conducted with ground stations and onboard receivers of the Doppler Orbitography and Radio-positioning Integrated by Satellite (DORIS) instrument system. An antenna mounted on the satellite points towards Earth to receive radio signals from the ground stations. The frequency shift caused by the Doppler effect is used to determine the distance between the ground stations and LEO satellites. A major product of the DORIS observations is the precise orbit determination with particular reference to altimetry and remote sensing.

Another relevant technology for precise orbit determination is satellite laser ranging (SLR). Despite the original application of SLR instruments being the derivation of geodetic parameters, they have great capabilities for precise orbit determination due to the high precision of the range measurements. In SLR, ground stations are continuously emitting laser pulses in the optical spectrum, and the LEO satellites are equipped with retro-reflectors to reflect the laser pulse. The basic observation is twice the laser time of flight between the ground station and a satellite. Due to the highly precise measurements, SLR is one of the main means of external validation of precise orbit determination (POD).

After the first assessment of space-borne GPS receivers onboard the Topex/Poseidon mission [98], GNSS became a well-established tracking system to provide LEO position, velocity, and time. The LEO orbit determination can be simply obtained by GNSS with single point positioning (SPP), where the solution relies on GNSS broadcast ephemerides and single-frequency pseudorange observations. As an advantage, the GNSS measurements observed on board the

TABLE 10. Examples of metrics used in ground segment optimisation problems.

Metric	Mathematical Formulations	Parameter Explanations	Reference
Carrier-to-noise ratio (C/N_0)	$C/N_{0_{db-Hz}} = 10\log_{10}(\frac{P_{carrier}}{P_{noise}})$	P is the power of the signal or noise, for the same system bandwidth and equivalent times	[49]
Geometric dilution of precision ($GDOP$)	$\Delta y = (H^T H)^{-1} H^T \Delta x$ $GDOP = \sqrt{tr\,(H^T H)^{-1}}$	Δy is the position offset H is the satellite geometry matrix Δx is the net error in the pseudorange value $tr(.)$ refers to the trace operator	[92], [95]
Link outage probability (LOP)	$LOP = \sum_{i=0}^{M-1} \binom{N}{i} A_i \times (1 - A_{N-i})$	M is the smallest number of required ground stations N is the total number of ground stations A_i is the availability of ground station i	[93], [96]
Rainfall attenuation (ITU-R Model)	$\gamma_R = kR^\alpha$	γ_R is the specific attenuation R is the rain rate k and α are frequency-based coefficients	[97]

satellite are sufficient for the LEO orbit determination. However, the precision of a few metres in dynamic solutions can pose a crucial issue to LEO-PNT navigation systems. A more sophisticated solution often incorporates precise GNSS products, carrier phase measurements, and dual-frequency data. The basic measurements are the zero-difference or double-difference observations. Zero-difference observation refers to the raw phase and pseudorange observations, as in precise point positioning (PPP). Double-difference approaches, on the other hand, use double-difference GNSS observations between the LEO satellite and ground stations or other LEO satellites. Following the continuous progress of GNSS technologies, the satellite-borne GNSS technique based on zero- or double-differences has gradually become the primary method of precise orbit determination for many satellite missions.

Most LEO missions carry out POD solutions offline, after downloading GNSS measurements and auxiliary data by the processing center on the ground. This latency depends on the time required for the downlink process and the time required to generate precise GNSS orbit and clock products. For a LEO-based navigation system that relies on spaceborne GNSS receivers, the latency of this downlink transmission and GNSS products generation can add a crucial burden to the real-time users, so that the LEO positioning technique must be selected according to the particular application of the satellite mission. A high-accuracy solution is based on hybrid systems utilising both GNSS and non-GNSS data. These hybrid solutions combine the best of both techniques, but they increase the time latency. On the other hand, a technique that has gained attention in recent years [99] is the use of precise GNSS algorithms with broadcast ephemerides. The GNSS-POD with broadcast ephemerides allows precise positioning without the need for complementary ground-to-space links, thus reducing the latency issue.

Among the positioning techniques to determine the satellite orbit, three typical solutions are: 1) kinematic, 2) dynamic, and 3) reduced-dynamic. The kinematic approach relies purely on geometrical determinations of the 3D coordinates. The LEO position is obtained epoch by epoch with no motion constraints. The main products are the coordinates, ambiguities, and receiver clocks. In the dynamic solution, the satellite orbit is constrained to a force model described by an equation of motion. The dynamic determinations are therefore governed by physical laws to represent a time-dependent orbit in which the quality depends on the gravitational and non-gravitational force models. The reduced-dynamic technique combines the kinematic and dynamic techniques by introducing a stochastic process in the representation of the trajectory. The residual of the estimations is adjusted within the orbit determination to help the compensation of remaining force model deficiencies [100]. Most often, empirical accelerations are included in the system in the radial, along-track, and cross-track (RAC) directions.

Table 11 provides an overview of the main POD options to be considered by the ground segment of a LEO-PNT system. It provides the type of input data (DORIS, SLR, or GNSS) as well as the positioning strategy, obtained solutions and overall accuracy level.

C. EPHEMERIDES

Defining the ephemerides that satisfy accuracy requirements for geodetic positioning is one of the most critical prerequisites of a LEO-PNT system. In SoO approaches, two-line elements (TLEs) are typically used to list a set of orbital elements and describe the LEO orbit with roughly approximations. In case of dedicated LEO-PNT systems, more accurate orbital descriptions are required.

Broadcast ephemeris models have been developed mainly for MEO and GEO satellites. Dedicated MEO-PNT systems typically uses ephemeris models based on Keplerian orbital elements [108]. They are broadcast to the user as legacy messages embedded in the system signal and can describe MEO satellites with an approximated user range error of 0.5 m [109]. This performance relies on the model fit errors, orbit determination and propagation errors.

Unlike MEO and GEO, the LEO satellites are much closer to the Earth. Therefore, they are affected to a greater extent by gravity and atmospheric drag forces. The legacy broadcast ephemeris models are therefore not capable of describing these complex orbital dynamics. Meng *et al.* [110], for instance, developed a broadcast model that takes into account the Keplerian elements being singular in some cases due to small eccentricities of the LEO orbits. The best results with this method were obtained using 22 Keplerian parameters in contrast to 16 in the legacy messages. The use of 16 parameters provided a user range error of around 4 to 18 m in LEO satellites at 800 km, while more coefficients could improve

the accuracy to the cm-level. In addition, the legacy messages of MEO orbit are described by arcs of two hours length. However, the authors in [110]–[112] have found reasonable accuracy only when describing LEO orbits with 20 to 30 min arc lengths.

Despite broadcast ephemeris are the most traditional way to compute the satellite orbit in navigation systems, the best efforts allow the provision of more precise products. The International GNSS Service (IGS) analysis centers provide ephemeris in the form of GNSS precise products. They allow precise orbit determination for the level of a few centimeters in near real time. Similar approaches can be conducted for LEO satellites, which may be relevant for applications requiring precise geodetic solutions. Current MEO GNSS satellites distribute precise orbital coordinates with a time resolution of 15 minutes. The best time step to distribute LEO precise products to users is not yet fully known.

D. SUMMARY OF GROUND SEGMENT CONSIDERATIONS

The most common metrics for obtaining the best location for a ground station were identified as signal availability level, number of visible satellites, GDOP, scintillation fade depth, ionospheric delay, and signal attenuation. Due to the proximity and speed of LEO satellites, metrics that depend on geometry and signal-to-noise ratios have been highlighted as the options with the best benefits in LEO-PNT systems.

There is no clear standard of how the ground segment should perform the POD of LEO satellites. A clear trend however is observed for techniques using onboard GNSS receivers. The most straightforward GNSS solution tends to use reduced-dynamic model, least-squares solvers, dual frequency signals with zero-difference phase and code observations. This can allow a 5 cm-level accuracy, which is a reasonable accuracy to develop broadcast ephemeris models.

In SoO approaches, TLE is the main ephemeris used for the orbit description, which are known to provide rough approximations of the satellites. In dedicated LEO-PNT approaches, more accurate models are required. However, instead of the broadcast ephemeris used in classical GNSS systems, the most recent advances show the necessity of dedicated ephemeris models. A viable option is to adapt the Keplerian-based ephemeris model used in GPS to incorporate more complex orbital dynamics. To this end, 22 Keplerian parameters with 20 to 30 min arc lengths can provide reasonable results in LEO satellites, in contrast to 16 parameters with 2 hours arc lengths of the legacy broadcast messages. Another option is to distribute precise products like IGS, so no Keplerian elements are broadcast. In such cases, more accurate solutions are expected, but the best time step to distribute the LEO coordinates is not yet fully known.

V. CHANNEL EFFECTS

Various channel effects can produce signal reflection, loss, refraction, diffraction, and polarisation shifts in LEO satellites. We summarise in this section the main channel effects that require different mitigation approaches from those used in classic GNSS.

A. PHASE WIND-UP EFFECT

Because of the electromagnetic nature of circularly polarised waves, antenna rotation on the transmitter or receiver side causes a phase variation. This phase variation, known as a phase wind-up, is reflected as a direct variation in the range measurements provided by the carrier phase. An antenna rotation of 360° generates an apparent range increase by a wavelength in the carrier phase. The impact of phase wind-up over GNSS L1 measurements refers to an error of about 0.19 m, so that phase wind-up must be corrected in precise solutions. At higher frequencies, the phase wind-up is smaller and, depending on the chosen frequency, can even be neglected for certain applications. The impact of neglecting the phase wind-up in precise positioning of LEO satellites using GNSS as transmitter has been pointed out in [113]; but to our knowledge, there is no discussion related to the phase wind-up originated by LEO satellite rotations, when the LEO satellites are the signal transmitter. In principle, faster panel rotations are expected for LEO satellites, resulting from the higher orbital speed.

B. IONOSPHERIC EFFECTS

The Earth's ionosphere is composed of positive ions and free electrons formed in the atmosphere [114], mainly by the ionization of neutral gases due to solar radiation. The number of electrically charged particles is large enough to cause refraction over several bands of RF signals. The ionosphere refers to the region between 50 to ∼2,000 km above the Earth's surface. Above the ionosphere, the electron density is low but still high enough to cause a significant refraction of the RF signals crossing a large portion of this layer, which is known as the plasmasphere.

Typical PNT receivers are designed to measure the propagation time of an RF signal. As the RF signal propagates through the ionosphere, it bends due to refraction effects, resulting in a longer time for the receiver to track the signal. This time delay is commonly referred as the ionospheric delay.

Since the ionosphere is a dispersive medium [115], [116], the RF signal propagates with distinct phase and group velocities. The refractive index is therefore applicable in two distinct formulations to represent the ionospheric delay over the RF signal (in metres):

$$I_g = \frac{40.3}{f^2}\int_s^r n_e ds \quad I_p = -\frac{40.3}{f^2}\int_s^r n_e ds \tag{5}$$

with I_g and I_p being the ionospheric group and phase delay, n_e the electron density, f the signal frequency, and $\int_s^r ds$ the geometric distance between the receiver r and satellite s.

As shown in equation (5), the ionospheric delay is proportional to the electron density and inversely proportional to the signal frequency. Higher frequencies are less affected by the ionospheric refractivity. In case of GPS L1 frequency,

TABLE 11. Survey of the LEO POD studies, including the POD method, accuracy and solution.

Ref.	Input Data	Positioning Strategy	Solution Obtained	Achieved Accuracy
[28]	Dual-frequency precise ephemerid GPS	POD using zero-difference observations in the GPS High-precision Orbit Determination Software Tools (GHOST)	Reduced-dynamic: position, velocity, atmospheric drag, solar radiation pressure, RAC accelerations, receiver clock, ambiguities; kinematic: position	reduced-dynamic: 2 cm kinematic: 4-5 cm
[99]	Dual-frequency broadcast ephemerid GPS, Galileo, Beidou	Real-time POD using zero-difference observations	Position, velocity, atmospheric drag, solar radiation pressure, RAC accelerations, receiver clock, ambiguities	8-10 cm
[101]	Dual-frequency broadcast ephemerid GPS	Real-time POD using zero-difference observations and pseudo-ambiguity	Position, velocity, atmospheric drag, solar radiation pressure, RAC accelerations, receiver clock, ambiguities	20–40 cm (position) 0.2–0.4 mm/s (velocity)
[102]	Dual-frequency precise ephemerid GPS	POD combining GPS and DORIS	Position, velocity, atmospheric drag, RAC accelerations, receiver clock, ambiguities	1.66-3.16 cm
[103]	Dual-frequency precise ephemerid simulated data	PPP aided by Keplerian elements	Position, velocity, gravity perturbation, three-body perturbation, atmospheric damping, solar pressure, and others	15 cm (position) 0.18 mm/s (velocity)
[104]	Doppler SLR normal point	Dynamic orbit determination to express forces acting on the satellite based on the Cowell numerical integration	Position, velocity, atmospheric drag, solar radiation pressure, RAC accelerations	DORIS-only: 7.69 cm SLR-only: 11.96 cm
[105]	Dual-frequency precise ephemerid GPS	POD using zero-difference observations POD using double-difference observations	Position, velocity, atmospheric drag, solar radiation pressure, RAC accelerations, receiver clock, ambiguities	zero-difference: 1-2.5 cm double-difference: 0.68-6.8 mm
[106]	Dual-frequency precise ephemerid GPS	POD using zero-difference observations in the PANDA software	Position, velocity, atmospheric drag, solar radiation pressure, RAC accelerations, receiver clock, ambiguities	2-10 cm
[107]	Dual-frequency real-time JPL eph. GPS	POD using zero-difference observations	Position, velocity, atmospheric drag, solar radiation pressure, RAC accelerations, receiver clock, ambiguities, and orbit manoeuvres	10-20 cm
[108]	SLR normal point	Dynamic orbit determination with the Cowell numerical integration in the GEODYN II software	Position, velocity, atmospheric drag	around 10 m (post-fit residuals)

for instance, the ionosphere can cause errors up to 15 m in the zenith direction [117]. The consideration of the ionospheric delay is therefore crucial for accurate positioning.

Several ionospheric models have been developed in the past decades to properly describe electron density for PNT applications with single-frequency systems. Traditional ionospheric models for real-time PNT applications are the Klobuchar model [118], currently used in GPS, the NeQuick [119], used by Galileo, and the BeiDou global broadcast ionospheric delay correction model [120]. Additionally, since 1998, the IGS is providing global ionospheric maps (GIMs) for more precise applications [121]. To date, the precision of the ionospheric delay estimation from the IGS remains around 1-2 metres [122]. The ionospheric delay provided by two-dimensional GIMs is counted from the ground up to the GNSS satellite height of around 20,000 km. Due to the topside ionosphere and plasmasphere, which represents 10% - 60% of the total ionospheric delay [123], the GIMs are not directly applicable in LEO-PNT systems. On these systems, the ionospheric delay will only affect the region up to the LEO orbit height and, hence, dedicated ionospheric models are necessary for single-frequency solutions.

In the case of sub-metre requirements, the use of isolated ionospheric models may not be sufficient. In such cases, PNT technology is more suitable if developed with two or more frequencies. Then, by means of a linear combination of the phase (or group) delays between the frequencies, it is possible to eliminate the first-order effects of the ionosphere. The first-order effect refers to approximately 99% of the refractivity [124]. The remaining effects of higher order can reach tens of centimetres. In GNSS applications, the higher-order effects can be eliminated by 3D ionospheric models to less than a few millimetres [124], so that similar ionospheric models can be adapted for use in the LEO-PNT technologies.

Diffractive effects pose a greater challenge to PNT technologies than ionospheric delays. As the signal's plane waves cross the ionosphere, small-scale irregularities in the electron density scatter the signal and result in rapid fluctuations of both phase and amplitude [125]. Interference patterns are then observed on the ground, inducing uncertainties in tracking loops due to multiple signal paths. The main effects observed on a receiver are associated with fading events, cycle slips, and loss of lock. Summing up all the challenges, the PNT system can completely fail to provide continuous operation during intense ionospheric scintillation, which occurs mainly at low and high latitudes during high solar activity. There are several studies on characterisation and mitigation of ionospheric scintillation in GNSS positioning (see [126] and references therein), but scintillation is still a limiting factor for sub-decimetre applications or for truly continuous operation. Any GNSS user at tropical or high-latitudes is particularly vulnerable to a positioning disruption during high solar activity.

The dependence of RF signals on ionospheric scintillation can be represented by [127]:

$$\sigma_\phi^{La} = \frac{f_{Lb}}{f_{La}}\sigma_\phi^{Lb} \quad S_4^{La} = \left(\frac{f_{Lb}}{f_{La}}\right)^{1.5} S_4^{Lb} \tag{6}$$

where σ_ϕ and S_4 stand for the phase and amplitude, respectively, of most common scintillation indexes, and *La* and *Lb* represent two L-band signals following the rule $f_{La} > f_{Lb}$.

Building on equation (6), we can understand that the higher the frequency, the lower the expected scintillation impact over the RF signals. This rule was validated in [128], showing that lower GPS frequencies (L2 and L5) suffer more intense scintillation than L1. Moreover, according to equation (6), for 2 GHz LEO-PNT system the effects of ionospheric scintillation are reduced by approximately 20% to 30% in comparison to GPS L1. For this reason, there is a great opportunity for the upcoming LEO-PNT systems to mitigate the ionospheric scintillations by increasing the signal frequency.

C. TROPOSPHERIC EFFECTS

The troposphere, often described as the neutral part of the Earth's atmosphere, is the closest atmospheric layer to the Earth's surface. The troposphere is stratified up to an altitude of about 50 km, where the refractive index is always greater than one. In consequence, tropospheric delays are expected in signals emitted by satellites on low Earth orbits. Variations in tropospheric delay depend on temperature, atmospheric pressure, humidity, and water vapor. This delay also depends on the receiver's geographic location as well as the satellite elevation angle relative to the receiver.

In terms of LEO-PNT systems, identical empirical models currently used in GNSS can be used for frequencies below 15 GHz. A possible gain is related to decorrelation of the troposphere during the estimation process. Indeed, the line of sight changes much faster for LEO transmitters than MEO ones. This geometric gain may greatly impact the time required to estimate the wet part of the tropospheric delay. Past studies [129], [130] have already observed the benefits of using LEO satellites to improve the PNT convergence time, but no studies have been developed so far to assess the time gain in the troposphere estimation.

D. TERRESTRIAL EFFECTS

LEO constellations can offer higher signal power than MEO. Nonetheless, signal quality and power are reduced by multipath effects when non-line-of-sight (NLoS) propagation dominates. Outdoor multipath may be dealt with in a similar way to classic GNSS systems. However, given the possibility of indoor positioning, we discuss the transmission of RF signals into buildings and introduce satellite-to-indoor channel models developed in this environment.

Unlike the reception of GNSS signals outdoors, where the line of sight (LoS) propagation dominates the communications between satellites and end user, indoor reception includes additional local interactions of materials and signals on spatial scales ranging from just a few metres to hundreds of metres. The smaller spatial scales allow direct experimentation with a building's system response to excitation by externally applied electromagnetic radiation. The use of the channel impulse response method has been central to several measurement and modelling activities [132], [133].

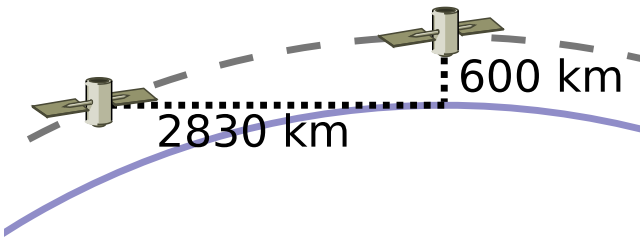

FIGURE 8. Two LEO satellites (altitude 600 km), one at nadir and the other near the horizon relative to a single receiver location on the ground. In this situation, the increased free space attenuation is approximately 13dB taking these two distances into consideration.

Results from observation and analysis activities have demonstrated that:

1) Indoor received signals vary as a function of the azimuthal and polar/altitude angles associated with the transmitter/receiver geometry [134], see Figure 8, and building materials (Figure 9).
2) Signal-level fluctuations can be as high as 30 dB over periods of several hundred milliseconds within various locations in a single room [135].
3) There is ''diffuse'' multipath activity with contributions of 20 to 35 wave fronts and associated delays up to 100 ns relative to the LoS signal [136].
4) Multipath delays indoors are smaller than those observed from the outdoor environment.

As shown in Figure 10, electromagnetic waves from LEO antennas travel a few hundred kilometres along the LoS. Waves may hit the different objects on earth (buildings, trees, cars, etc.) and propagate into different directions due to scattering, diffraction, and reflections. Furthermore, waves can penetrate the building roof or walls, resulting in losses that depend on the construction material (Figure 9). In general, wave propagation indoors will be mainly in the form of multipath, and the impulse response of multipath wireless channels can be modelled as [137]:

$$h(t;\tau) = \sum_i \alpha_i(t)\, e^{-j\theta_i(t)} \delta\left((t - \tau_i(t))\right) \tag{7}$$

The summation is performed over the waves' path components. Each path has its specific gain α_i, angle θ_i, and delay τ_i. Due to the associated uncertainty, it is convenient to consider the parameters of the channel impulse response as random processes. The signal strength usually decreases inversely with the distance between the transmitter and receiver (in free space, the power gain obeys an inverse square law). However, due to the multipath environment, it could easily be shown that the power attenuation with distance can be higher than 2, and is usually between 3 and 5 or even more.

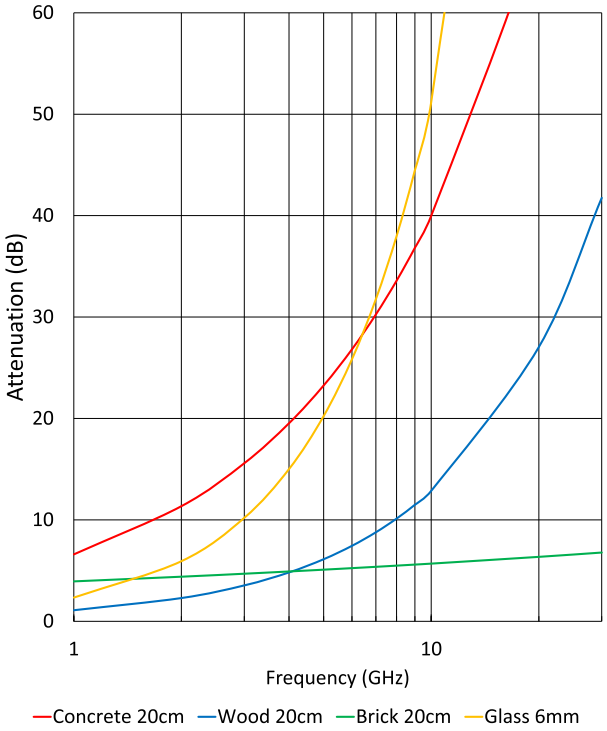

FIGURE 9. RF signal attenuation caused by absorption characteristics of common building materials (as a function of wavelength, GHz). [131].

In some exceptional indoor scenarios, the power-law factor may be less than 2; this is known as the waveguide effect, but a power-law factor of 3 to 4 is more common in indoor applications. In a real environment, the channel model depends on a vast number of factors. Hence, it is infeasible to find an accurate deterministic model that could be used to express the general channel model, and therefore it is more realistic to use a stochastic model to express the multipath channel uncertainties. The models best known for this purpose are the Rician, Rayleigh, and Nakagami-m channel models.

The Rician channel model is used for a strong LoS beam beside multipath components, as shown in Figure 10. When the LEO satellite is on a small horizontal angle, the electromagnetic wave might propagate indoors with a strong LoS path through the windows. On the other hand, the Rayleigh channel is a useful model in a rich multipath environment without a dominant LoS path. The Nakagami-m channel is a scalable model that is capable of modelling a wide class of fading channel conditions, and it fits the empirical data well [138].

Generally speaking, the received signal power can be modelled with

$$P_r = \frac{G_{rt}\sigma\eta}{d^{\alpha}}P_t \tag{8}$$

where P_r and P_t are the received and transmitted power respectively, G_{rt} is the multiplication of transmitter and receiver antenna gains, d is the distance between the transmitter and receiver, and σ is the shadowing losses. Shadowing can be modelled as a random process with log-normal

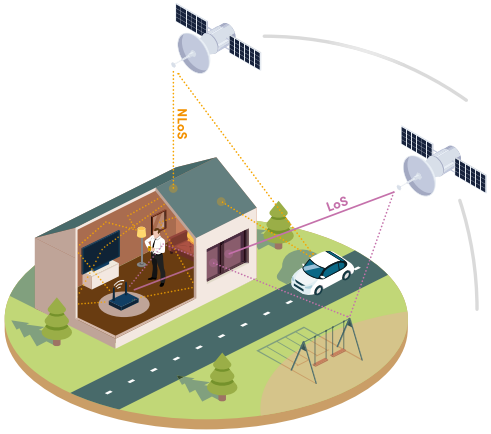

FIGURE 10. Conceptual depiction of LoS and NLoS signals propagating from LEO satellites to an indoor environment.

distribution, but passed through a narrow band linear filter. Shadowing represents slow losses such as those caused by entering buildings or being behind a big object. On the other hand, η represents a small-scale fading (i.e., fast-changing received signal characteristic due to small changes in the receiver location). The small-scale factor generally results from multipath. It can be modelled as the square of a random process (Rayleigh, Rician, or Nakagami-m) passed through a linear filter representing the Doppler filter (i.e., it creates the duration period of the time correlation due to the Doppler spread), and α is the exponent factor of the distance power decay.

E. SUMMARY OF CHANNEL EFFECTS CONSIDERATIONS

We first identified that faster antenna rotations are expected in LEO satellites than in MEO orbits. As a result, phase wind-up effects will likely produce fast artificial range variations, which can be mitigated by the adoption of lower wavelengths. We also find that most ionospheric models for GNSS positioning do account the ionospheric delay from the ground up to approximately 20,200 km. There is a large region between approximately 800 and 20,200 km of the extra ionospheric content in such models, which requires dedicated ionospheric models for single-frequency systems. Another point is that ionospheric scintillation has been one of the main barriers to achieving sub-decimeter accuracy for precise GNSS positioning. Therefore, there is a great opportunity for upcoming LEO-PNT systems to mitigate ionospheric scintillation by increasing signal frequency. New LEO-PNT systems can also provide a significant means for mitigating the tropospheric effects. Due to the faster speed of LEO compared to MEO satellites, the spatial-temporal decorrelation of the tropospheric delay estimation is better achieved as the line of sight geometry changes faster. LEO-PNT systems can also provide several benefits for indoor positioning. Given the close proximity to the Earth, LEO signals are received indoors at a higher power. But the carrier frequency plays an important

TABLE 12. Impact of channel effects over a LEO-PNT system using SoO, modified payload, or new LEO-PNT.

	SoO	Modified Payload	New LEO-PNT
Phase Wind-Up	negligible	depends on system frequency. Centimetre error on L-band.	depends on system frequency. Centimetre error on L-band.
Ionospheric Refraction	negligible	depends on system frequency. Metric error on L-band	depends on system frequency. Metric error on L-band.
Ionospheric Scintillation	impact not investigated, but depends on system frequency	impact not investigated, but depends on system frequency	depends on system frequency. Loss of lock and metric error on L-band.
Tropospheric Effects	negligible	Metric error	Metric error
Multipath	Depends on AoA. Can reach several hundred Hertz.	1/4 of wavelength. Centimetre error on L-band.	1/4 of wavelength. Centimetre error on L-band.

role, since higher frequency bands suffer from a higher attenuation, especially indoors. The trade-offs between higher path losses due to increased carrier frequencies and smaller path losses due to close proximity to Earth need to be carefully investigated.

Table 12 summarises the current general understanding of the impact of signal channel effects in the case of SoO, modified payloads or new dedicated signals.

VI. USER SEGMENT

The user segment consists of RF receivers and antennas that receive PNT signals, process the measurements, and provide solutions. From a wide range of users, this section focuses on the PNT user segment.

A. RECEIVER CONSIDERATIONS

A general navigation receiver architecture, comprises a radio front-end and components for processing base band signals and navigation data. Initial signal reception and conversion into a digitized sample is performed in the radio front-end. The remaining components of the radio front-end amplify the signal above the noise, and downconvert it to an intermediate frequency (IF). The analog to digital converter and signal processing chain completes the receiver. To form a general understanding of LEO-PNT receivers, this section is separated into two parts: receiver design for 1) a LEO system that is dedicated to PNT, and 2) a Doppler measurement-based system.

1) DEDICATED SYSTEMS

A dedicated LEO-PNT system contains navigation parameters embedded in the RF signal. The receiver is responsible for decoding the navigation messages in a customized device. Dedicated LEO-PNT systems do not yet exist globally, but there are aspirations in this direction. Satelles [139] and Xona Space System [140] are two examples of companies that serve as guides to the necessary assumptions for a dedicated LEO-PNT user receiver. Receiver assumptions are concerned with signal design, as decoding a signal is a user receiver's task. A reasonable option is to follow the design of a GNSS signal since we can benefit from the vast expertise in this field. A dedicated signal such as this is composed of a minimum of two frequencies and three layers. As previously mentioned, two frequencies allow for ionospheric corrections. Three layers refer to the carrier wave, code and data modulations superimposed on it.

Accuracy is the key advantage of a dedicated system over an opportunistic one. Xona Space Systems plans to use this to their advantage and develop a LEO-PNT service, called Xona Pulsar, for the high-reliability sector of autonomous vehicles. Three aspects determine the accuracy gain of a dedicated LEO-PNT signal compared with an exclusive carrier positioning method: the code gain, the transmitted data, such as ephemeris, and the timing reference:

1) *Code* refers to known modulation onto the carrier wave identifying the specific transmitting satellite. A local replica of this signal is reproduced in the user receiver for correlation between the two signals. Acquisition and tracking of weaker signals are enabled by correlation. This is known as code gain. Such higher acquisition sensitivity benefits pseudorange measurements in a weak signal environment. An example of this is the satellite time and location (STL) service by Satelles. STL is hosted on Iridium satellites, and its significance lies in the adjustments to the transmitted signal. The beginning of the STL transmission is marked by the STL burst. Performing correlation with this burst enables even weaker signals to be detected within the user receiver [139]. In a 13-floor building, the STL code gain results in a C/N_0 between 35 and 55 dB-Hz, compared to GNSS in an unobstructed environment [141]. The STL burst is the functional equivalent of PRN code in GNSS.
2) *Data* refers to the information transmitted in the signal. In the case of GNSS, this is the navigation message, or ephemeris. A dedicated LEO-PNT system would also need to transmit such navigational information to perform precision positioning measurements. The navigation parameters need to be adjusted specifically to the LEO environment, with likely additions of new parameters. The user receiver must then be adjusted to the respective symbol duration and pass on the parameters to the navigation filter.
3) *Pseudorange* measurements rely on high-precision timing and frequency information. GNSS satellites contain highly accurate, and expensive atomic clocks for their timing broadcasts. A GNSS receiver can be used to provide an external timing reference. However, if the LEO-PNT system is to be independent of GNSS, and no atomic clock timing broadcasts are available, other timing references are needed. Satelles compared temperature compensated crystal oscillators (TCXOs), oven-controlled crystal oscillators (OCXOs), and a rubidium disciplined clock [139]. It was concluded that OCXOs result in a better timing output than TCXOs, and rubidium clocks perform best out of the three. A compact rubidium clock was shown to achieve sub-500 ns maximum time interval error (MTIE). That is

the maximum error within a seven-day time interval without further ground corrections. An OCXO with ground-station-issued corrections obtained sub-100 ns. Ultimately, user receiver precision requirements determine whether a rubidium clock is necessary or a cheaper OCXO will suffice.

There is a significant change in LoS for a LEO satellite near the horizon compared to its zenith position. The shortest LoS is between the satellite's zenith position and the user receiver. Thus, the least path loss and highest received signal power are obtained for a LoS satellite. This might be considered in the user receiver as a setting in the SDR of high angles in the elevation mask [142].

2) DOPPLER LEO-PNT

In Doppler LEO-PNT systems, COTS components are frequently used in combination with signals of opportunity (SoO). Thus, an additional element for frequency downconversion may be required when using K-band frequencies. In addition to downconversion, the most significant differences between LEO-PNT and GNSS are in the positioning framework, assumptions concerning navigation parameters, and the implementation of the acquisition and tracking loops. There is no need to use correlators, as SoO contains no code signal to be replicated and matched in a user receiver. An ephemeris message is not decoded either. Furthermore, the most suitable receiver architecture is based on the requirements of the user environment.

The final positioning solution is obtained by a navigation filter. Extended Kalman filters (EKFs) are common, and they are explored further in Section VI-C, along with other positioning solutions. However, it is necessary to know which navigation information is missing to substitute it accordingly. This is done by adjusting the acquisition and tracking loops, as well as using additional measurement components, such as altimeters. Tracking loops in Doppler positioning generally lay out of the PLL [143], or they are implemented based on a Kalman filter [144], [145]. The former type of tracking loop is commonly used in combination with a known signal structure. The latter type may be adjusted to also track customized navigation observable based on signals of publicly unknown structure [144].

A positioning framework based solely on Doppler measurements is presented by [146]. The state of the user receiver is determined by three spatial components, three velocity components, clock offset, and clock drift. Thus, the user receiver requires eight processing channels to perform eight simultaneous carrier Doppler shift measurements. A carrier Doppler shift measurement accuracy of $0.01\,\mathrm{m\,s^{-1}}$ in terms of equivalent range-rate accuracy needs to be achieved to obtain positioning solutions comparable to GNSS [146]. However, timing accuracy is still stated to be the most challenging aspect.

Due to the lack of ephemeris data in the Doppler positioning method, the satellite's status is generally obtained by feeding the receiver and navigation filter by public TLE files [145]. The vertical resolution of Doppler measurements is poor, but the accuracy can be improved with altimeters [144]. Another common addition is an inertial measurement unit (IMU) or an inertial navigation system (INS) [1]. These may also be used for velocity measurements of a dynamic user receiver.

Propagation errors caused by the ionosphere and troposphere are typically neglected for simplicity. The order of magnitude of these errors is significantly smaller than the velocity errors of TLE files, but the effects are noticeable in the positioning accuracy.

Further errors are introduced by receiver and transmitter clocks. Appropriate models for their behaviour are, therefore, necessary. A common simplified method is using white Gaussian noise errors with constant clock drift with known variance. The timing or frequency reference used in the receiver determines the accuracy of the actual clock state. Timing accuracy on the order of milliseconds is realistic [146], making this the critical accuracy aspect for receiver considerations using Doppler positioning. However, if the satellite has access to precise atomic clock timing and sends frequent updates, it is possible to ease the accuracy requirements in the user receiver clock [147].

Another consideration is the number of tracking and processing channels. Using multiple constellation signals, it might be favourable to implement several independent channels requiring multiple user radio front-ends. The bandwidth is dependent on the respective signal frequency too. The Doppler shift of a LEO signal varies significantly during an overhead pass, such that a broad bandwidth commonly needs to be sampled [144]. Devices that collect the samples and perform such post-processing are shown in [1] and [144].

The user environment determines the priorities in the receiver architecture. A weak signal environment may require a focus on acquisition sensitivity through targeted improvements to the acquisition loop [148]. Moreover, a LEO receiver may be used to aid a GNSS receiver's acquisition search space [149]. Both of these approaches likely focus on processing low frequencies, such as L-band or lower, as they are less attenuated by obstructions compared to high frequencies, such as K-bands [146]. The advantage of K-band frequencies lies in the signal transmissions of LEO mega-constellations. Their vast numbers of satellites may be able to provide consistent global signal availability. To benefit from this, a user receiver may require additional downconversion in the radio front-end [144].

Table 13 summarises Doppler-LEO-PNT receiver configurations with simulated and experimental user positioning results. Common to all of them is a customised SDR approach. The simulated accuracy results outperform the real-scenario user positioning partially because of simplified conditions of the simulations. More satellites are assumed to be available for measurements, and more precise knowledge of satellite states is presumed. Initial experiments with multiple Starlink satellites support a trend towards higher

accuracy. The best user positioning performance, with an accuracy around 7.7 m, is obtained using six Starlink satellites, an altimeter, and a customised SDR setup [144].

B. PNT TECHNIQUES

There are several techniques to obtain PNT solutions after the received data is processed. SoO techniques are mostly applied using single receiver stations with configurations and accuracy levels already mentioned in Table 13. This section focuses on dedicated LEO-PNT approaches. For the sake of simplicity, we categorise the distinct PNT techniques into two types: using one or multiple receiver stations.

1) PNT TECHNIQUES WITH ONE RECEIVER STATION

Single-receiver PNT techniques have received increased attention due to their simplicity for users, who need only one receiver. Two popular techniques used in GNSS are single point positioning (SPP) and precise point positioning (PPP).

SPP is the basic GNSS mode. It is based on single-frequency pseudorange observations, broadcast ephemeris, and simple correction models for the ionosphere and troposphere. This is the usual method for civil GNSS applications, reaching an accuracy of a few metres. Santerre *et al.* [152], for instance, achieved an accuracy of 5 to 20 meters in a challenging urban environment. LEO-PNT systems aiming for similar accuracy with SPP require a dedicated signal for the generation of pseudoranges, in addition to a dedicated broadcast ephemeris and embedded ionospheric model.

The main drivers for PPP are the carrier phase measurements, aided by precise models to describe satellite orbit, clocks, troposphere, ionosphere, and terrestrial effects. Since the carrier phase has an accuracy of a few millimetres, the PPP accuracy depends on external models, which encompass orbital errors, clock errors, channel effects, receiver errors, and terrestrial effects. For GNSS, real-time and post-processed products are continuously provided to properly mitigate these systematic errors. Such products are generated through the best efforts of an international community sharing open data processed by a series of institutes that maintains global and regional GNSS networks. The computations to produce relevant products are coordinated by the IGS analysis centers. PPP can achieve an accuracy of a few centimetres. To provide this robust position solution with PPP, a LEO-PNT system needs to provide similar precise products, which calls for worldwide cooperation.

SPP and PPP can be applied using distinct measurement combinations to benefit from the internal signal proprieties. PPP approaches solely using single-frequency (SF) measurements may provide metric solutions [153]. For more accurate PPP, SF combinations often help the solver, despite the existence of cm-level SF-PPP when using robust ionospheric models [122]. In dual-frequency (DF) systems, cm-level PPP solutions are possible using a mix of linear combinations in the estimation process [154], such as ionospheric-free, wide-lane, narrow-lane and Geometry-free combinations.

Usually, standalone GPS allows a stable PPP solution after 30 to 60 minutes. LEO-PNT technologies, however, can improve real-time PPP and convergence time by several minutes when aided by GNSS [129], [130]. In the most recent LEO-PNT simulations [129], [130], PPP convergence time dramatically shortened to about 6 minutes when using only LEO satellites. Even faster, 3 minute convergence time was feasible when using a LEO constellation-augmented by classic GNSS. All solutions were in the cm-level, demonstrating the great benefits of LEO satellites to PPP techniques.

2) PNT TECHNIQUES WITH MULTIPLE RECEIVER STATIONS

PNT techniques with multiple receiver stations often require one or a few base stations with known coordinates for the determination of unknown coordinates of the target receiver stations (rover stations). There are two major methods: 1) computing differential corrections or 2) forming measurement combinations relative to a base station.

1) **differential positioning**: point positioning is first performed for the base station to compute corrections. Then, another point positioning is applied to the rover station. The rover's point positioning is improved by the corrections computed for the base station, reaching an accuracy that depends on how far they are apart. Assuming that the rover is close enough to the base, similar errors are expected between the stations. This is called differential GNSS (DGNSS) and it is applied in GNSS to obtain dm-level accuracy [155], [156] without the need of external precise models and products. The technique can be further improved with the virtual reference station (VRS) concept [157].
2) **relative positioning**: the main idea is to transform measurements of the distance between transmitter and receiver into distances between the base and rover stations, the so-called baselines. Relative positioning offers advantages over single-receiver PNT techniques. The baselines are formed using measurement combinations of single-difference (SD) and double-difference (DD) to eliminate several errors intrinsic to the measurements. The basic assumption is that two receivers are simultaneously observing the same satellites. By subtracting the corresponding pseudorange (or phase) measurements between the receivers and/or satellites, clock errors, atmospheric effects, phase wind-up and the initial non-integer part of the phase bias are eliminated/mitigated. The DD combination is the most preferable observable in GNSS positioning techniques aiming to solve phase biases. It benefits from noise and error mitigation of the original measurements, being the main driver of several state-of-the-art GNSS software solutions, such as BERNESE [158], which provides millimetre-level solutions.

To our knowledge, there are no simulations to assess the performance of PNT techniques with multiple receivers for the upcoming LEO-PNT systems. However, we expect that

TABLE 13. Survey of user receivers in Doppler positioning. Ephemeris is obtained via TLEs in all references, except [150]. The accuracy is stated in the user positioning root mean square error (RMSE).

Receiver Configuration	User Velocity	Constellation	Measurement	Estimator	Accuracy in m	Ref.
Equipped with an altimeter	Static	Orbcomm	Pseudorange rate	EKF	11.38 (2D, simulated) , 358 (2D, experimental), (both including height info.)	[145]
Equipped with INS	Dynamic	Globalstar, Orbcomm, Iridium, Starlink	Pseudorange rate	EKF	10.5 (simulated GOI), 10.1 (simulated Starlink)	[151]
Equipped with INS	Dynamic	Orbcomm	Pseudorange rate	EKF	416.5 (experimental)	[151]
KF-loops in SDR	Static	Starlink	Carrier phase	Least Square	7.7 including height info. (2D), 25.9 without height info. (2D), 33.5 without height info. (2D) (all experimental)	[144]
Multi-constellation switching mode	Static	Iridium, Orbcomm	Pseudorange rate	EKF	177.1 (3D, experimental), 132 (2D, experimental)	[143]
Quadratic square accumulating Doppler Shift	Static	Iridium	Doppler-shift	Least Square	400 (3D, experimental), 163/ 198 including height info. (2D, experimental)	[148]
Equipped with INS	Dynamic	Iridium	Pseudorange and range rate	KF	200 m to 1 km (simulated)	[1]
Mobile receiver and base station	Dynamic	Globalstar, Orbcomm, Iridium, Starlink	Differential Doppler measurement with AOA	KF	100 m within 2 km of base station (simulated)	[150]

satellite clocks can be eliminated in the DD formation, so that a looser design can be defined in the space segment. As a counterpart, the user needs at least two receivers in the field campaigns. Therefore, higher costs are expected on the user side. To mitigate user cost, the ground segment must be implemented with several reference stations to serve as base stations with known coordinates, which is already the case for GNSS. The maintenance of the DGNSS or DD receiver networks is a responsibility of national and international institutes. They maintain continuously operating reference stations (CORS) by combining the efforts of hundreds of government, academic, and private organizations. The cost to implement a similar worldwide service, while a great impediment to applying strategies similar to GNSS and obtaining the most precise PNT solutions, is still doable.

C. PNT ESTIMATORS

Even though LEO satellites have the potential for complementary PNT services, the current LEO satellites are not optimal for PNT. They can be smaller and of lower quality than MEO satellites. The lack of actual LEO-PNT satellites favours using SoO in addition to navigation signals. Some obstacles can be mitigated with more advanced estimation algorithms to select and fuse LEO signals and additional information. This subsection reviews the estimation and optimisation algorithms for LEO PNT: LS, Kalman Filters (KF), Particle Filters (PF), Factor Graphs (FG) and Particle Swarm Optimisation (PSO).

1) LEAST SQUARES

The LS method is simple, computationally efficient, and therefore useful for LEO satellite positioning problems. Because the LS solution is not robust against erroneous data, it is crucial to detect and remove incorrect observations before using them. The standard method in the GNSS domain is the receiver autonomous integrity monitoring (RAIM) algorithm. In LEO positioning, some more advanced techniques have been developed. For example, an unsupervised clustering method for removing NLOS signals was used before solving the terminal position with LS [159].

2) KALMAN FILTER

Many Doppler-based LEO positioning solutions have been developed based on KF reaching close to 10 m accuracy [144], [145], [176]. They often combine Doppler observations of SoO with IMU values [177].

- **Extended Kalman Filter** (EKF): Kalman algorithm is an iterative recursive filtering method for predicting optimal states in linear state-space systems considering additive white Gaussian noise [164]. The algorithm proceeds by utilising prior knowledge to estimate the posterior states, calculate the Kalman gain, and determine the residual error due to the mismatch between the generated ground truth and the measurements. Then the new state mean and covariance vectors are calculated and fed to the next iteration [165]–[167]. An extended Kalman filter is a non-linearly approximated version of the ordinary linear Kalman filter to estimate states in nonlinear dynamic systems [168], as illustrated in Figure 11. In EKF, the state transition and the measurement matrices from the linear Kalman filter are replaced by non-linear state transition functions $f(.)$ and non-linear measurement function $h(.)$, respectively, to map the algorithm through Gaussian distribution to work in non-linear conditions.
- **Unscented Kalman filter** (UKF): UKF employs the sigma point transformation to model the non-linear state transition function of the system and linearize it via the unscented transform [167], [169]. The UKF algorithm utilises additional points besides the distribution mean, while EKF approximation relies only on one point, the mean. UKF selects these weighted points (i.e., the sigma points) plus the mean for better mapping the non-linear space. This procedure is called the unscented transform. There are other sigma point Kalman filters, such as Cubature (CKF).

TABLE 14. Positioning estimators summary.

Algorithm	Accuracy	Speed	Properties	Ref.
Iterative LS	high	moderate	static, iterative, can converge to local minimum	[49], [160]
Direct LS	moderate	high	static, partly iterative	[161]–[163]
wLS / ML	high	moderate	static, iterative, flexible, can converge to local minimum	[49], [160]
KF	moderate	high	dynamic, linear, recursive, parametric	[164]–[167]
EKF	moderate	high	dynamic, recursive, parametric	[168]
UKF	moderate	high	dynamic, recursive, parametric	[167], [169]
PF	moderate	moderate	dynamic, recursive, non-parametric	[170], [171]
FGO	high	low	dynamic, iterative parametric	[172], [173]
PSO	high	low	static, iterative, non-parametric, global optimisation	[174], [175]

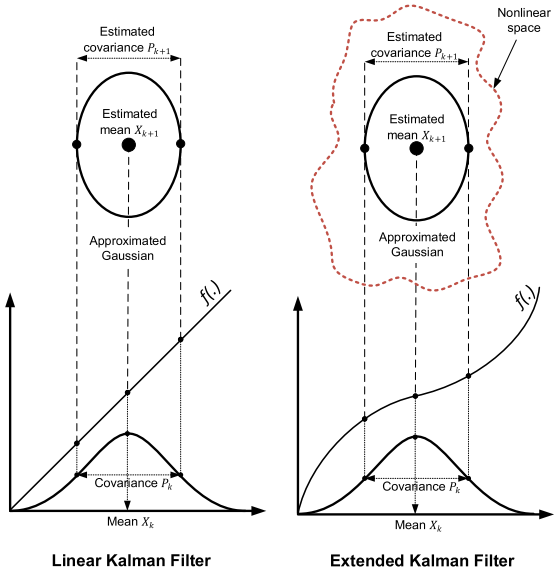

FIGURE 11. Illustration depicting EKF approximation for non-linear systems, adapted from [178].

3) PARTICLE FILTER (PF)

PF models the posterior distribution of the location with a swarm of discrete samples, known as particles. The particle cloud can represent many kinds of distributions, and the noise models related to observations and dynamic state model can also be arbitrary [179]. The basic implementations of PF have certain limitations, but there are many advanced versions, described for example by Elfring et.al [171]. PF has been used for LEO carrier tracking [180] and RADAR-based object tracking applications [181]. The flexible noise model makes the PF applicable to LEO positioning problems.

4) FACTOR GRAPH (FG)

Factor graph is one of the newest Bayesian filtering methods. Unlike with a Kalman filter, all past states can be used to calculate the maximum posterior probability iteratively. In the FGO model, the joint distribution is factorised as multiplication of marginal distributions, which can be represented graphically as a factor graph. The previous navigation and sensor calibration states are represented as nodes, and the edges are the sensor observations represented as factors. The iterative solution utilising previous states and observations improves the accuracy and robustness of the position estimate at the cost of additional computational resources. Real-time solution is still possible if the sampling frequency is not too high [173], [182]. Some early publications have found FG useful in mitigating multipath effects [183] and for sensor fusion combining GPS, IMU, and stereo vision [184]. Even though there are few examples using FG for LEO satellite navigation, the flexibility and additional accuracy of FGs make them potentially attractive. Since FGs are often used in simultaneous location and mapping (SLAM) applications, they are particularly suitable for simultaneous tracking and navigation (STAN), where the uncertain orbit of LEO satellite is refined while carrying out positioning.

5) GLOBAL OPTIMISATION METHODS

Particle swarm optimisation (PSO), originally introduced in [185] and [174], is a global optimisation strategy, i.e., it strives for finding the global optimum in possibly non-linear, non-convex search space. PSO can be used for solving the static positioning problem when local optima can cause problems; otherwise, iterative LS is more efficient. The PSO method as such cannot utilise the dynamic model, but it is sometimes combined with dynamic methods such as PF [175]. PSO has been applied in the LEO navigation domain to satellite selection [186] and faulty signal avoidance [187].

6) SENSOR FUSION

Fusion-based positioning methods combine the measurements of multiple sensors to further refine the PNT solution, maximising the information content, mitigating the sources of errors and thus reaching higher precision [178]. The main steps of sensor fusion are described in Figure 12, where data from a group of sensors are locally processed using their corresponding solvers (algorithms), then the output is weighed and later combined with other sensors (fused) globally using the proper fusion scheme to produce the final optimal solution.

Sensor fusion as a computational procedure can take the architecture of three distinct fusion schemes: a) loosely

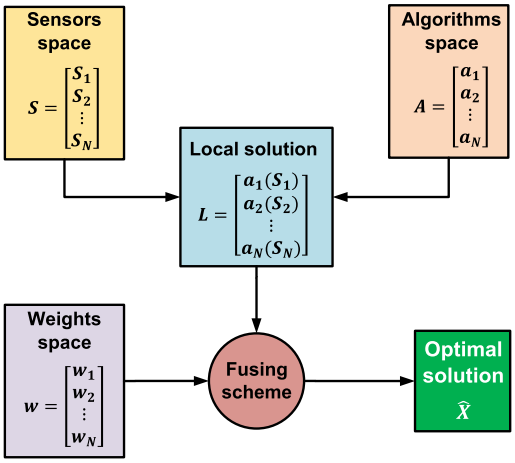

FIGURE 12. Sensor fusion framework, adapted from [178], [188].

coupled (LC), b) tightly coupled (TC), and c) ultra tightly coupled (UTC). As stated by [189], in GNSS, LC is the simplest type among the three architectures that provides the essential redundancy based on the duplicated information in situations of good visibility (four satellites) to achieve high accuracy. TC is widely adopted because it provides better accuracy and is less susceptible to jamming, in addition to maintaining navigation in situations of poor visibility (fewer than four satellites). While in UTC, the tracking loop of GNSSs is assisted with an accompanying SDR loop that matches and smooths between the locally generated signal and the actual received signal.

LEO satellites have great potential to benefit from sensor fusion with other technologies to leverage PNT-based applications. The fusion of LEO positioning data with other assisting positioning technologies would exploit the link budgets of existing LEO constellations to provide PNT data at no additional cost or complication to onboard hardware technology. As the conceptual proposal released by [190] states, it is possible to get low-cost PNT solutions using the existing broadband LEO satellites in orbit, such as the Starlink constellation, by fusion with GNSS. The authors concluded that the resources of the Starlink constellation, which already enable coverage to most of the world's population (< 60° latitude), could be reallocated to consume 0.8% of downlink capacity, 0.36% of energy capacity, and a negligible percentage of uplink capacity to sacrifice an increase of approximately 0.1 dB in maximum pointing loss.

Another concept is the STAN framework [191]. It is a LEO-based method in a realistic simulation environment to localise an unmanned aerial vehicle (UAV) where GNSS signal is denied, by interfacing with the Globalstar, Iridium, Orbcomm, and Starlink constellations. Unlike GNSS, which periodically send information about their clock offsets and current location, the STAN framework tracks the LEO satellite states by exploiting their signals to determine their pseudoranges and Doppler measurements, then feeds the drawn data to the vehicle's onboard inertial navigation sensors (INS). The optimal fusion estimation is then performed via EKF to localise the UAV. Simulation results showed an absolute error of 9.9 m and an RMSE of 10.5 m with Globalstar, Iridium, and Orbcomm, while with Starlink the LEO/INS method achieved an error of 9.8 m and RMSE of 10.1 m.

The introduction of massive multiple-input multiple-output (mMIMO) concept into LEO-PNT is recently discussed by [55], [192], [193]. The concept comprises the use of massive arrays of beamforming antennas hence exploiting the multipath. This setup has numerous advantages which can enhance the LEO-based localization, especially in the inevitable events of superposition where the UT is spotted by multiple beamformed loops. In addition, mMIMO is capable of extending the coverage area on Earth per each LEO satellite by adopting space-time block coding which maximizes the number of beneficiary UTs.

D. SUMMARY OF USER SEGMENT CONSIDERATIONS

We have found potential in the development of PNT receivers as the whole LEO-based positioning sector is developing at a fast pace. However, there is still a distinction between high versus low accuracy. Signals of opportunity receivers require lower complexity than dedicated LEO-PNT solutions, at the cost of providing lower positioning performance, as their main tasks are offering good communication and sensing performance, rather than good positioning performance. Dedicated LEO-PNT systems, on the other hand, are more accurate, but limited in providing only PNT (and possibly sensing) applications. The accuracy discrepancy is getting smaller as more commercial efforts are filling this market and providing better satellite visibility and higher coverage on Earth. However, the best way to compete with GNSS technology is still uncertain, but is leaning towards working in cooperation with it rather than as a competitive solution. The PPP solution appears to be the most benefited among the GNSS techniques, but simulations are still required to assess the LEO-PNT systems when using multiple ground stations. Regarding estimators, LC is the simplest type of sensor fusion that provides the necessary redundancy based on the duplicated information, while TC is less susceptible to jamming and tolerates poor coverage better. The STAN methods may be beneficial for LEO PNT when the orbits are not as accurate as in the case of GNSS.

VII. SIMULATION EXAMPLES

Several simulator manufacturers offer LEO satellite simulation options. This section provides an overview of the main hardware and software simulators.

A. HARDWARE SIMULATORS

The hardware-based LEO simulators are a prime example of tools to facilitate LEO-PNT development. They are space segment-based, which means that they can simulate GNSS measurements of receivers onboard LEO satellites. Ground segment-based simulators using LEO satellites as

transmitters, on the other hand, are rare according to the authors' knowledge.

- **Spirent simulator**: Spirent simulators are commonly used to simulate GNSS signals from various constellations and receiver configurations. Although most simulators are designed primarily for MEO-based GNSS signal generation considering the receiver on the ground, the Spirent GSS9000 series can simulate receivers onboard LEO satellites by describing the LEO trajectory with high dynamic motion and ultra-low latency. For example, GSS9000 can simulate relative velocities of 120 km/s, including one or two versatile RF outputs. The user can use both RF outputs at the same time: one to generate available GNSS signals, and the other to generate novel PNT signals replaying in-phase & quadrature (IQ) data in conjunction with the GNSS simulator.
- **LabSat SatGen**: even though SatGen is a software simulator, it requires a LabSat device to play the simulated data as RF signals. SatGen software enables users to generate IQ data depending on their trajectory, which can be replayed on the Labsat GNSS simulator. Researchers can utilize SatGen to build a scenario that simulates extremely high dynamic situations, allowing them to test receiver performance onboard LEO satellites.

B. SOFTWARE SIMULATORS

Various commercial or open-access software simulators currently exist for LEO modelling at different architectural levels, but none of the current ones are providing a full-chain solution, to the best of the authors' knowledge. According to the segment in the propagation chain, we can divide these software simulators into several subsections:

1) SPACE-SEGMENT SIMULATORS

- **MATLAB**: for modelling the satellite orbits and 3D coordinates motion, we can use the MATLAB Satellite Communications Toolbox (introduced in release 2020a). This toolbox contains useful functions to model and propagate satellite orbits and constellations, visualise the propagated orbits, and analyse line-of-sight access between satellites and ground stations. For propagating the orbits, different perturbation models can be used: two-body (assumes the Earth is a sphere and no perturbations besides gravity), SGP4 (taking into consideration Earth oblateness and atmospheric drag) and SDP4 (which, besides the perturbations considered by SGP4, additionally includes solar and lunar gravity). MATLAB Satellite Communications Toolbox model both 3D position and velocity, which is useful for Doppler-based measurements.
- **poliastro**: poliastro is an open source Python library that allows the simulation of astrodynamics and orbital mechanics, with a focus on ease of use, speed, and quick visualisation. Several useful functions can be utilised to perform the computation of classical orbital elements, numerical orbit propagation, and orbital manoeuvres. The orbit propagation can be computed considering a two-body force, gravitational effects due to Earth oblateness, atmospheric drag, and several propagators, such as the Cowell numerical integration.
- **STK**: System Tool Kit (STK) by Analytical Graphics is a software simulation tool for analysing land, sea, air, and space assets within a high-fidelity environment model and time-dynamic three-dimensional simulation. It enables the modelling, analysis, and interaction of mission objects and targets. STK is widely used in aerospace applications for the analysis of satellites, orbits, and space environment. It supports multiple satellite and constellation missions. Additionally, it enables access calculations for ground stations and areas of interest. STK provides real-time 2D and 3D visualisation from the land, sea, air, and space components using high-resolution terrain, imagery, and RF environment. Advanced modules include satellite subsystem modelling, space environment effects, and conjunction analysis [194].
- **GMAT**: The General Mission Analysis Tool (GMAT) is a free and open source software application developed by NASA in collaboration with public and private contributors, as well as industry. It is a multi-mission space mission design, optimisation, and navigation software package that supports missions ranging from low Earth orbit to lunar, libration points, and deep space. It contains orbit propagators, spacecraft models, and thruster models. It facilitates analysis by generating reports and plots. The GMAT tool is widely used to support missions, educate students, and conduct outreach [195], [196].
- **SaVoir**: SaVoir by Taitus Software is a multi-satellite swath planner initially developed for the European Space Agency to aid in rapidly evaluating acquisition opportunities with a satellite and sensor combination across any region of interest. This application displays Earth and other celestial bodies in 2D and 3D, as well as a vast number of images of the Earth's surface with current or expected clouds. The initial set of orbits and models for major remote sensing satellites and constellations that has already been integrated can be updated online. Multiple earth orbiting satellites can be simulated in near real time [197]–[199].
- **Savi**: SaVi is a cross-platform, open source software program for analysis and visualisation of satellite constellations. Satellite orbits can be created and analysed in two and three dimensions. The software enables the user to monitor satellite coverage for Earth-orbiting satellites. The software includes a variety of existing satellite constellations, including Iridium, Globalstar, GPS, and Galileo. [87], [198].

2) WIRELESS CHANNEL SIMULATORS

- **QuaDRiGa**: One option for modelling a realistic wireless channel is by using the QuaDRiGa [200], [201] framework. QuaDRiGa is a MATLAB-based software developed by Fraunhofer HHI that enables modelling wireless channels by generating realistic radio channel impulse responses for system-level simulations. It is very flexible, allowing different simulation layouts by modifying some variables. QuaDRiGa offers a wide operating range (carrier frequencies comprised between 0.5 GHz and 100 GHz) for the simulations. In addition, QuaDriga offers the possibility to modify the transmitter and receiver position, orientation, and movement profile (with specific focus on satellite orbit propagation). Additionally the antenna type to be used in both receiver and transmitter can be selected among a few options, or or a customised. The specific channel models for satellite application are downlink oriented [202]. QuaDRiGa framework contains the following ready-to-use downlink specific channel scenarios: rural, sub-urban, urban, dense urban, and as LoS and NLoS propagation conditions. Each of these scenarios contains specific features (e.g., number of multipath and scattering object's size) according to its nature.

3) GROUND- AND USER-SEGMENT SIMULATORS

The authors are not aware of any commercial or open source simulators in the existing literature to simulate LEO-PNT dedicated or opportunistic signals; however, some works have recently developed their own techniques: [27], [130], [203], [204].

VIII. COMMERCIAL PERSPECTIVES

To form an understanding of commercial endeavours for the upcoming LEO-PNT systems, business model typology can be used. They help to understand the whole ecosystem where the firms work and how they create value for other firms as well as end users. The business model can be applied, including four components [205]. The first component is ''product/service'', that refers to how a firm is using LEO-PNT-enabled technologies to provide new services. As an example, the US start-up company Satelles provides PNT-based services complementary to the GNSS to allow better performance quality and operational resilience. Their services can be used to increase safeguarding time stamps in trading or using satellite time and location (STL) when GNSS signals are disrupted or manipulated. The second component,''value network'', refers to the key actors (firms, authorities, customers, partners, etc.) enabling LEO-PNT services. Satelles has several partners in their value network that together enable the implementation of the services. These partners include solution providers and original equipment manufacturers incorporating STL technology. The third component, ''value delivery'', demonstrates how value is delivered to and between various actors in the value network. In the case of Satelles, the value is delivered through partners to end users, such as data centers and teleoperators. The fourth component, ''revenue model'', shows how the value that a firm offers to end users, customers, and partners, can generate financial income. The Satelles' revenue model is based on the services they provide for customers and end users.

As accurate PNT is a key requirement for a variety of markets and industries, upstream and downstream firms are currently launched or planned, such as Satelles, Future Navigation, and Xona Space Systems [19]. The upstream market in the new space industry is typically considered to include hardware manufacturing firms, whereas the downstream segment typically includes data analytic service providers [206]. Based on these two segments, the overall GNSS market is rapidly evolving. Currently, the business models for PNT services largely depend on the existing GNSS systems. Since LEO-PNT system developments are moving at a fast pace, new business models for both start-ups and established firms in upstream as well as downstream markets are expected in the near future.

IX. CONCLUSION

In this survey, several requirements to build a new LEO-PNT system have been analysed. An extensive literature review has shown considerations to implement the signal design, space segment, ground segment, and user segment. Advantages and drawbacks of various instruments and techniques were discussed in order to detect possible options to materialise LEO-based navigation systems. Our investigation has not led to a clear recommendation of preferable options in every single aspect of the LEO-PNT system since there are very few works that have provided simulations in the current literature. Future simulations are therefore required to define optimal signal designs, constellations, atmospheric models, and PNT techniques. Nevertheless, dedicated LEO-PNT systems, as adopted by Xona Space Systems, are a viable option to bring relevant gains to the current PNT solutions and lead to innovative business models for both start-ups and established companies.

We have also analysed relevant material of the current stage and future direction in LEO-PNT systems. The rapid evolution in the space segment has led to a significant reduction of cost in the launch, deployment and maintenance of small satellites. At the same time, the literature review over simulation results have shown that GNSS technologies, which are now exclusively based on MEO and GEO satellites, can be improved by LEO satellites in terms of geometry and signal reception power. These are important measures for improving urban and indoors navigation, setting LEO-PNT as a possible solution to solve current challenges in the field of navigation, positioning and timing.

REFERENCES

[1] H. Benzerrouk, Q. Nguyen, F. Xiaoxing, A. Amrhar, A. V. Nebylov, and R. Landry, ''Alternative PNT based on iridium next LEO satellites Doppler/INS integrated navigation system,'' in *Proc. 26th Saint Petersburg Int. Conf. Integr. Navigat. Syst. (ICINS)*, May 2019, pp. 1–10.

[2] A. Nardin, F. Dovis, and J. A. Fraire, "Empowering the tracking performance of LEO PNT by means of meta-signals," in *Proc. IEEE Int. Conf. Wireless for Space Extreme Environments (WiSEE)*, Oct. 2020, pp. 153–158.
[3] R. Morales-Ferre, E. S. Lohan, G. Falco, and E. Falletti, "GDOP-based analysis of suitability of LEO constellations for future satellite-based positioning," in *Proc. IEEE Int. Conf. Wireless Space Extreme Environments (WiSEE)*, Oct. 2020, pp. 147–152.
[4] D. Egea-Roca, J. A. López-Salcedo, G. Seco-Granados, and E. Falletti, "Comparison of several signal designs based on chirp spread spectrum (CSS) modulation for a LEO PNT system," in *Proc. 34th Int. Tech. Meeting Satell. Division Inst. Navigat. (ION GNSS+)*, Oct. 2021.
[5] C. Fernandez-Prades, L. L. Presti, and E. Falletti, "Satellite radiolocalization from GPS to GNSS and beyond: Novel technologies and applications for civil mass market," *Proc. IEEE*, vol. 99, no. 11, pp. 1882–1904, Nov. 2011.
[6] E. A. Bretz, "Precision navigation in European skies," *IEEE Spectr.*, vol. 40, no. 9, p. 16, Sep. 2003.
[7] Y.-F. Tsai and K.-S. Low, "Performance assessment on expanding SBAS service areas of GAGAN and MSAS to Singapore region," in *Proc. IEEE/ION Position, Location Navigat. Symp. (PLANS)*, May 2014, pp. 686–691.
[8] J. L. Grubb, "The traveler's dream come true (satellite personal communication)," *IEEE Commun. Mag.*, vol. 29, no. 11, pp. 48–51, Nov. 1991.
[9] O. B. Osoro and E. J. Oughton, "A techno-economic framework for satellite networks applied to low Earth orbit constellations: Assessing starlink, oneweb and kuiper," *IEEE Access*, vol. 9, pp. 141611–141625, 2021.
[10] K. Çelikbilek, Z. Saleem, R. Morales Ferre, J. Praks, and E. S. Lohan, "Survey on optimization methods for LEO-satellite-based networks with applications in future autonomous transportation," *Sensors*, vol. 22, no. 4, p. 1421, Feb. 2022.
[11] S. Abulgasem, F. Tubbal, R. Raad, P. I. Theoharis, S. Lu, and S. Iranmanesh, "Antenna designs for CubeSats: A review," *IEEE Access*, vol. 9, pp. 45289–45324, 2021.
[12] A. H. Lokman, P. J. Soh, S. N. Azemi, H. Lago, S. K. Podilchak, S. Chalermwisutkul, M. F. Jamlos, A. A. Al-Hadi, P. Akkaraekthalin, and S. Gao, "A review of antennas for picosatellite applications," *Int. J. Antennas Propag.*, vol. 2017, Apr. 2017, Art. no. 4940656.
[13] R. Rajan, R. Vedanayagi, and S. Renukadevi, "Antenna designs for amateur band low Earth orbit (LEO) satellites—A review," *Int. J. Res. Eng. Appl. Manage.*, vol. 4, no. 5, pp. 245–259, Sep. 2018.
[14] P. Petropoulou, E. T. Michailidis, A. D. Panagopoulos, and A. G. Kanatas, "Radio propagation channel measurements for multi-antenna satellite communication systems: A survey," *IEEE Antennas Propag. Mag.*, vol. 56, no. 6, pp. 102–122, Dec. 2014.
[15] O. Kodheli, E. Lagunas, N. Maturo, S. K. Sharma, B. Shankar, J. F. M. Montoya, J. C. M. Duncan, D. Spano, S. Chatzinotas, S. Kisseleff, J. Querol, L. Lei, T. X. Vu, and G. Goussetis, "Satellite communications in the new space era: A survey and future challenges," *IEEE Commun. Surveys Tuts.*, vol. 23, no. 1, pp. 70–109, 4th Quart., 2021.
[16] T. G. Reid, T. Walter, P. K. Enge, D. Lawrence, H. S. Cobb, G. Gutt, M. O'Connor, and D. Whelan, "Navigation from low earth orbit: Part 1: Concept, current capability, and future promise," in *Position, Navigation, and Timing Technologies in the 21st Century: Integrated Satellite Navigation, Sensor Systems, and Civil Applications*, vol. 2. Wiley, 2020, pp. 1359–1379, doi: 10.1002/9781119458555.ch43a.
[17] Z. Z. M. Kassas, *Navigation From Low-Earth Orbit*. Hoboken, NJ, USA: Wiley, 2021, pp. 1381–1412.
[18] J. Bouwmeester, and J. Guo, "Survey of worldwide pico- and nanosatellite missions, distributions and subsystem technology," *Acta Astron*, vol. 67, nos. 7–8, pp. 854–862, 2010.
[19] E. Kulu, "Satellite constellations-2021 industry survey and trends," in *Proc. 35th Annu. Small Satell. Conf.*, 2021, pp. 1–20.
[20] F. Davoli, C. Kourogiorgas, M. Marchese, A. Panagopoulos, and F. Patrone, "Small satellites and cubesats: Survey of structures, architectures, and protocols," *Int. J. Satell. Commun. Netw.*, vol. 37, no. 4, pp. 343–359, Jul./Aug. 2019.
[21] G. Curzi, D. Modenini, and P. Tortora, "Large constellations of small satellites: A survey of near future challenges and missions," *Aerospace*, vol. 7, no. 9, p. 133, Sep. 2020.
[22] R. S. Jakhu and J. N. Pelton, *Small Satellites and Large Commercial Satellite Constellations*. Cham, Switzerland: Springer, 2017, pp. 357–378.
[23] G. Denis, D. Alary, X. Pasco, N. Pisot, D. Texier, and S. Toulza, "From new space to big space: How commercial space dream is becoming a reality," *Acta Astronautica*, vol. 166, pp. 431–443, Jan. 2020.
[24] H. Ge, B. Li, S. Jia, L. Nie, T. Wu, Z. Yang, J. Shang, Y. Zheng, and M. Ge, "LEO enhanced global navigation satellite system (LeGNSS): Progress, opportunities, and challenges," *Geo-Spatial Inf. Sci.*, vol. 25, no. 1, pp. 1–13, Jan. 2022.
[25] S. Liu, Z. Gao, Y. Wu, D. W. Kwan Ng, X. Gao, K.-K. Wong, S. Chatzinotas, and B. Ottersten, "LEO satellite constellations for 5G and beyond: How will they reshape vertical domains?" *IEEE Commun. Mag.*, vol. 59, no. 7, pp. 30–36, Jul. 2021.
[26] N. Saeed, A. Elzanaty, H. Almorad, H. Dahrouj, T. Y. Al-Naffouri, and M.-S. Alouini, "CubeSat communications: Recent advances and future challenges," *IEEE Commun. Surveys Tuts.*, vol. 22, no. 3, pp. 1839–1862, 3rd Quart., 2020.
[27] X. Li, Z. Jiang, F. Ma, H. Lv, Y. Yuan, and X. Li, "LEO precise orbit determination with inter-satellite links," *Remote Sens.*, vol. 11, no. 18, p. 2117, Sep. 2019.
[28] J. van den IJssel, J. Encarnação, E. Doornbos, and P. Visser, "Precise science orbits for the Swarm satellite constellation," *Adv. Space Res.*, vol. 56, no. 6, pp. 1042–1055, Sep. 2015.
[29] I. Gorbatyy, "Particularities of the amplitude shift keying signal spectrum calculation," in *Proc. Int. Conf. 'Modern Problems Radio Eng., Telecommun. Comput. Sci.' (TCSET)*, 2008, pp. 475–476.
[30] F. Xiong, "M-ary amplitude shift keying OFDM system," *IEEE Trans. Commun.*, vol. 51, no. 10, pp. 1638–1642, Oct. 2003.
[31] T. Anfray, A. Mottet, J.-J. Bonnefois, R. Cousty, S. Mariojouls, A. Laurent, H. Porte, J. Hulin, W. Atitallah, J. Hauden, T. Schmitt, and P. Berceau, "Assessment of the performance of DPSK and OOK modulations at 25 Gb/s for satellite-based optical communications," in *Proc. IEEE Int. Conf. Space Opt. Syst. Appl. (ICSOS)*, Oct. 2019, pp. 1–6.
[32] I. D. Portillo, B. G. Cameron, and E. F. Crawley, "A technical comparison of three low earth orbit satellite constellation systems to provide global broadband," *Acta Astronautica*, vol. 159, pp. 123–135, Jun. 2019.
[33] P. Ferrand, M. Maso, and V. Bioglio, "High-rate regular APSK constellations," *IEEE Trans. Commun.*, vol. 67, no. 3, pp. 2015–2023, Mar. 2019.
[34] K. P. Liolis, R. D. Gaudenzi, N. Alagha, A. Martinez, and A. G. I. Fàbregas, "Amplitude phase shift keying constellation design and its applications to satellite digital video broadcasting," in *Digital video*, F. D. Rango, Ed. Rijeka, Croatia: IntechOpen, 2010, ch. 20.
[35] Y. Qian, L. Ma, and X. Liang, "Symmetry chirp spread spectrum modulation used in LEO satellite Internet of Things," *IEEE Commun. Lett.*, vol. 22, no. 11, pp. 2230–2233, Nov. 2018.
[36] A. Roy, H. B. Nemade, and R. Bhattacharjee, "Symmetry chirp modulation waveform design for LEO satellite IoT communication," *IEEE Commun. Lett.*, vol. 23, no. 10, pp. 1836–1839, Oct. 2019.
[37] Y. Qian, L. Ma, and X. Liang, "The performance of chirp signal used in LEO satellite Internet of Things," *IEEE Commun. Lett.*, vol. 23, no. 8, pp. 1319–1322, Aug. 2019.
[38] T. Wu, D. Qu, and G. Zhang, "Research on Lora adaptability in the LEO satellites Internet of Things," in *Proc. 15th Int. Wireless Commun. Mobile Comput. Conf. (IWCMC)*, Jun. 2019, pp. 131–135.
[39] M. K. Simon, "On the bit-error probability of differentially encoded QPSK and offset QPSK in the presence of carrier synchronization," *IEEE Trans. Commun.*, vol. 54, no. 5, pp. 806–812, May 2006.
[40] M. N. Pachery and M. R. Bhatnagar, "Double differential modulation for LEO-based land mobile satellite communication," *IEEE Trans. Aerosp. Electron. Syst.*, vol. 56, no. 4, pp. 3339–3346, Aug. 2020.
[41] H. Ezzat, A. Hassan, and M. El-Soudani, "M-ary continuous phase frequency shift keying transmissions through nonlinear channels in additive Gaussian noise and cochannel interferences," in *Proc. Int. Zurich Seminar Digit. Commun., Electron. Circuits Syst. Commun.*, Mar. 1990, pp. 495–511.
[42] M. Rahmani and B. G. Family, "Design and implementation of a GMSK baseband modem for UHF radio modem," in *Proc. Int. Power Syst. Conf. (PSC)*, Dec. 2019, pp. 33–36.
[43] T. Venugopal and S. Radhika, "A survey on channel coding in wireless networks," in *Proc. Int. Conf. Commun. Signal Process. (ICCSP)*, Jul. 2020, pp. 0784–0789.
[44] J. Jin Kong and K. K. Parhi, "Interleaved cyclic redundancy check (CRC) code," in *Proc. 37th Asilomar Conf. Signals, Syst. Comput.*, vol. 2, Nov. 2003, pp. 2137–2141.
[45] D. J. C. MacKay, "Fountain codes," *IEE Proc. Commun.*, vol. 152, no. 6, pp. 1062–1068, Dec. 2005.

[46] R. G. Gallager, "Low-density parity-check codes," *IRE Trans. Inf. Theory*, vol. 8, no. 1, pp. 21–28, Jan. 1962.
[47] B. Tahir, S. Schwarz, and M. Rupp, "BER comparison between convolutional, turbo, LDPC, and polar codes," in *Proc. 24th Int. Conf. Telecommun. (ICT)*, May 2017, pp. 1–7.
[48] L. Wang, Z. Lü, X. Tang, K. Zhang, and F. Wang, "LEO-augmented GNSS based on communication navigation integrated signal," *Sensors*, vol. 19, no. 21, p. 4700, Oct. 2019.
[49] E. D. Kaplan and C. J. Hegarty, Eds., *Understanding GPS: Principles and Applications*, 2 ed. Norwood, MA, USA: Artech House, 2006.
[50] P. Angeletti and R. De Gaudenzi, "A pragmatic approach to massive MIMO for broadband communication satellites," *IEEE Access*, vol. 8, pp. 132212–132236, 2020.
[51] M. Caus, A. Perez-Neira, and E. Mendez, "Smart beamforming for direct LEO satellite access of future IoT," *Sensors*, vol. 21, no. 14, p. 4877, Jul. 2021.
[52] B. Falkner, H. Zhou, A. Mehta, and A. Modigliana, "Flat panel interlaced shared aperture antenna array for LEO Ka-band high throughput satellite communication applications," in *Proc. IEEE Int. Symp. Antennas Propag. USNC-URSI Radio Sci. Meeting (APS/URSI)*, Dec. 2021, pp. 777–778.
[53] G. He, X. Gao, L. Sun, and R. Zhang, "A review of multibeam phased array antennas as LEO satellite constellation ground station," *IEEE Access*, vol. 9, pp. 147142–147154, 2021.
[54] K. Y. Zhong, Y. J. Cheng, H. N. Yang, and B. Zheng, "LEO satellite multibeam coverage area division and beamforming method," *IEEE Antennas Wireless Propag. Lett.*, vol. 20, no. 11, pp. 2115–2119, Nov. 2021.
[55] R. M. Ferre, E. S. Lohan, H. Kuusniemi, J. Praks, S. Kaasalainen, C. Pinell, and M. Elsanhoury, "Is LEO-based positioning with mega-constellations the answer for future equal access localization?" *IEEE Commun. Mag.*, vol. 60, no. 6, pp. 40–46, Jun. 2022.
[56] C. D. Brown, *Elements of Spacecraft Design*. Reston, VA, USA: American Institute of Aeronautics and Astronautics, Jan. 2002.
[57] P. Fortescue, G. Swinerd, and J. Stark, *Spacecraft Systems Engineering*. Hoboken, NJ, USA: Wiley, 2011.
[58] T. P. Garrison, M. Ince, J. Pizzicaroli, and P. A. Swan, "Systems engineering trades for the IRIDIUM constellation," *J. Spacecraft Rockets*, vol. 34, no. 5, pp. 675–680, Sep. 1997.
[59] T. Wekerle, J. B. Pessoa Filho, L. E. V. L. D. Costa, and L. G. Trabasso, "Status and trends of smallsats and their launch vehicles—An up-to-date review," *J. Aerosp. Technol. Manage.*, vol. 9, no. 3, pp. 269–286, 2017.
[60] R. A. de Carvalho, J. Estela, and M. Langer, *Nanosatellites: Space and Ground Technologies, Operations and Economics*. Hoboken, NJ, USA: Wiley, 2020.
[61] B. Yost, S. Weston, G. Benavides, F. Krage, J. Hines, S. Mauro, S. Etchey, K. O'Neill, and B. Braun, "State-of-the-art small spacecraft technology," NASA, Washington, DC, USA, Tech. Rep. NASA/TP-20210021263, 2021.
[62] J. D. Liddle, A. P. Holt, S. J. Jason, K. A. O'Donnell, and E. J. Stevens, "Space science with cubesats and nanosatellites," *Nature Astron.*, vol. 4, no. 11, pp. 1026–1030, Nov. 2020.
[63] S. K. Rao, "Advanced antenna technologies for satellite communications payloads," *IEEE Trans. Antennas Propag.*, vol. 63, no. 4, pp. 1205–1217, Apr. 2015.
[64] A. Babuscia, B. Corbin, M. Knapp, R. Jensen-Clem, M. Van de Loo, and S. Seager, "Inflatable antenna for cubesats: Motivation for development and antenna design," *Acta Astronautica*, vol. 91, pp. 322–332, Oct. 2013.
[65] R. Florencio, J. A. Encinar, R. R. Boix, V. Losada, and G. Toso, "Reflectarray antennas for dual polarization and broadband telecom satellite applications," *IEEE Trans. Antennas Propag.*, vol. 63, no. 4, pp. 1234–1246, Apr. 2015.
[66] Y. Rahmat-Samii, V. Manohar, and J. M. Kovitz, "For satellites, think small, dream big: A review of recent antenna developments for cubesats," *IEEE Antennas Propag. Mag.*, vol. 59, no. 2, pp. 22–30, Apr. 2017.
[67] P. A. Warren, J. W. Steinbeck, R. J. Minelli, and C. H. Mueller, "Large, deployable S-band antenna for a 6U cubesat," in *Proc. 29th AIAA/USU Conf. Small Satell.*, 2015, pp. 1–7.
[68] T. M. Braun, *Satellite Communications Payload and System*. Hoboken, NJ, USA: Wiley, 2021.
[69] P. Li, J. Liang, and X. Chen, "Study of printed elliptical/circular slot antennas for ultrawideband applications," *IEEE Trans. Antennas Propag.*, vol. 54, no. 6, pp. 1670–1675, Jun. 2006.
[70] F. J. Gonzalez Martinez, "Performance of new GNSS satellite clocks," Ph.D. thesis, Karlsruher Institut für Technologie, Fakultät für Bauingenieur-, Geo- und Umweltwissenschaften (BGU), Karlsruhe, Germany, 2014.
[71] P. Berceau, M. Taylor, J. Kahn, and L. Hollberg, "Space-time reference with an optical link," *Classical Quantum Gravity*, vol. 33, no. 13, Jul. 2016, Art. no. 135007.
[72] H. Zhang, H. Herdian, A. T. Narayanan, A. Shirane, M. Suzuki, K. Harasaka, K. Adachi, S. Yanagimachi, and K. Okada, "29.4 ultra-low-power atomic clock for satellite constellation with 2.2×10^{-12} long-term Allan deviation using cesium coherent population trapping," in *IEEE Int. Solid-State Circuits Conf. (ISSCC) Dig. Tech. Papers*, Feb. 2019, pp. 462–464.
[73] D. Van Buren, P. Axelrad, and S. Palo, "Design of a high-stability heterogeneous clock system for small satellites in LEO," *GPS Solutions*, vol. 25, no. 3, p. 105, Jul. 2021.
[74] K. M. Larson, N. Ashby, C. Hackman, and W. Bertiger, "An assessment of relativistic effects for low Earth orbiters: The GRACE satellites," *Metrologia*, vol. 44, no. 6, pp. 484–490, Nov. 2007.
[75] J. Wertz, *Mission Geometry: Orbit and Constellation Design and Management: Spacecraft Orbit and Attitude Systems*. Portland, OR, USA: Microcosm Press, 2001.
[76] V. A. Chobotov, *Orbital Mechanics*, 3rd ed. Reston, VA, USA: American Institute of Aeronautics and Astronautics, Jan. 2002.
[77] D. Beste, "Design of satellite constellations for optimal continuous coverage," *IEEE Trans. Aerosp. Electron. Syst.*, vol. AES-14, no. 3, pp. 466–473, May 1978.
[78] B. Gavish and J. Kalvenes, "The impact of satellite altitude on the performance of LEOS based communication systems," *Wireless Netw.*, vol. 4, pp. 119–213, Feb. 1998.
[79] G. Dai, X. Chen, M. Wang, E. Fernández, T. N. Nguyen, and G. Reinelt, "Analysis of satellite constellations for the continuous coverage of ground regions," *J. Spacecraft Rockets*, vol. 54, no. 6, pp. 1294–1303, Nov. 2017.
[80] E. Lansard, E. Frayssinhes, and J.-L. Palmade, "Global design of satellite constellations: A multi-criteria performance comparison of classical Walker patterns and new design patterns," *Acta Astronautica*, vol. 42, no. 9, pp. 555–564, May 1998.
[81] T. J. Lang and W. S. Adams, "A comparison of satellite constellations for continuous global coverage," in *Mission Design & Implementation of Satellite Constellations* (Space Technology Proceedings). The Netherlands: Springer, 1998, pp. 51–62.
[82] D. Mortari, M. P. Wilkins, and C. Bruccoleri, "The flower constellations," *J. Astron. Sci.*, vol. 52, nos. 1–2, pp. 107–127, Mar. 2004.
[83] M. E. Avendaño, J. J. Davis, and D. Mortari, "The 2-D lattice theory of flower constellations," *Celestial Mech. Dyn. Astron.*, vol. 116, no. 4, pp. 325–337, Aug. 2013.
[84] J. J. Davis, M. E. Avendaño, and D. Mortari, "The 3-D lattice theory of flower constellations," *Celestial Mech. Dyn. Astron.*, vol. 116, no. 4, pp. 339–356, Aug. 2013.
[85] D. Arnas, D. Casanova, E. Tresaco, and D. Mortari, "3-dimensional necklace flower constellations," *Celestial Mech. Dyn. Astron.*, vol. 129, no. 4, pp. 433–448, Dec. 2017.
[86] D. Arnas, D. Casanova, and E. Tresaco, "2D necklace flower constellations," *Acta Astronautica*, vol. 142, pp. 18–28, Jan. 2018.
[87] L. Wood, "SaVi: Satellite constellation visualization," 2022, *arXiv:1204.3265*.
[88] L. Globalstar, "Description of the globalstar system," Globalstar, Covington, LA, USA, Tech. Rep. GS-TR-94-0001, 2000.
[89] Globalstar. (2016). *Terrestrial Use of the 2473–2495 MHz Band for Low-Power Mobile Broadband Networks; Amendments to Rules for the Ancillary Terrestrial Component of Mobile Satellite Service Systemsystem, Attachment a: Technical Information to Supplement Schedule*. Accessed: Dec. 20, 2021. [Online]. Available: https://docs.fcc.gov/public/attachments/FCC-16-181A1.pdf
[90] M. J. Evans and T. D. Maclay, "Mission design of the orbcomm constellation," in *Mission Design Implement. Satell. Constellations*, J. C. van der Ha, Ed. Amsterdam, The Netherlands: Springer, 1997, pp. 103–112.
[91] O. Gupta, "Iridium NEXT SensorPODs: Global access for your scientific payloads," in *Proc. AIAA/USU Conf. Small Satell.*, 2011, pp. 1–5.
[92] A. A. M. Shah Sadman and M. Hossam-E-Haider, "Study of GNSS parameters and environmental factors over Bangladesh intended for selecting ideal ground station location for SBAS," in *Proc. 2nd Global Conf. Advancement Technol. (GCAT)*, Oct. 2021, pp. 1–6.
[93] A. Cornejo, S. Landeros-Ayala, J. M. Matias, and R. Martinez, "Applying learning methods to optimize the ground segment for HTS systems," in *Proc. IEEE 11th Latin Amer. Symp. Circuits Syst. (LASCAS)*, Feb. 2020, pp. 1–4.

[94] X. Liu, Y. Ge, C. Zhao, B. Li, and R. Zhou, "A study on global monitoring station optimization deployment method based on navigation satellite quadruple observing coverage," in *Proc. Int. Conf. Commun., Inf. Syst. Comput. Eng. (CISCE)*, May 2021, pp. 394–399.
[95] C.-S. Chen, Y.-J. Chiu, C.-T. Lee, and J.-M. Lin, "Calculation of weighted geometric dilution of precision," *J. Appl. Math.*, vol. 2013, Oct. 2013, Art. no. 953048.
[96] C. Fuchs and F. Moll, "Ground station network optimization for space-to-ground optical communication links," *IEEE/OSA J. Opt. Commun. Netw.*, vol. 7, no. 12, pp. 1148–1159, Dec. 2015.
[97] *Specific Attenuation Model for Rain for Use in Prediction Methods*, document P.2040-2 (09/2021), ITU Recommendation, International Telecommunication Union, United Nations, 2021.
[98] T. P. Yunck, W. I. Bertiger, S. C. Wu, Y. E. Bar-Sever, E. J. Christensen, B. J. Haines, S. M. Lichten, R. J. Muellerschoen, Y. Vigue, and P. Willis, "First assessment of GPS-based reduced dynamic orbit determination on TOPEX/Poseidon," *Geophys. Res. Lett.*, vol. 21, no. 7, pp. 541–544, Apr. 1994.
[99] A. Hauschild and O. Montenbruck, "Precise real-time navigation of LEO satellites using GNSS broadcast ephemerides," *Navigation*, vol. 68, no. 2, pp. 419–432, 2021.
[100] D. Arnold, O. Montenbruck, S. Hackel, and K. Sośnica, "Satellite laser ranging to low Earth orbiters: Orbit and network validation," *J. Geodesy*, vol. 93, no. 11, pp. 2315–2334, Nov. 2019.
[101] F. Wang, X. Gong, J. Sang, and X. Zhang, "A novel method for precise onboard real-time orbit determination with a standalone GPS receiver," *Sensors*, vol. 15, no. 12, pp. 30403–30418, Dec. 2015.
[102] Y. Zhao, F. Yu, and N. Xu, "PPP augmentation and real-time precise orbit determination for LEO satellites," in *Proc. 36th Chin. Control Conf. (CCC)*, Jul. 2017, pp. 5937–5941.
[103] Q. Kong, J. Guo, Y. Sun, C. Zhao, and C. Chen, "Centimeter-level precise orbit determination for the HY-2A satellite using DORIS and SLR tracking data," *Acta Geophys.*, vol. 65, pp. 1–12, Jan. 2017.
[104] D. Gu, B. Ju, J. Liu, and J. Tu, "Enhanced GPS-based GRACE baseline determination by using a new strategy for ambiguity resolution and relative phase center variation corrections," *Acta Astronautica*, vol. 138, pp. 176–184, Sep. 2017.
[105] Z. Qile, L. Jingnan, and G. Maorong, "High precision orbit determination of CHAMP satellite," *Geo-Spatial Inf. Sci.*, vol. 9, no. 3, pp. 180–186, Jan. 2006.
[106] Y. T. Yoon, M. Eineder, N. Yague-Martinez, and O. Montenbruck, "TerraSAR-X precise trajectory estimation and quality assessment," *IEEE Trans. Geosci. Remote Sens.*, vol. 47, no. 6, pp. 1859–1868, Jun. 2009.
[107] Y.-R. Kim, E. Park, D. Kucharski, H.-C. Lim, and B. Kim, "The challenge of precise orbit determination for STSAT-2C using extremely sparse SLR data," *Adv. Space Res.*, vol. 57, no. 5, pp. 1159–1176, Mar. 2016.
[108] P. Steigenberger, O. Montenbruck, and U. Hessels, "Performance evaluation of the early CNAV navigation message," *Navigation*, vol. 62, no. 3, pp. 219–228, Sep. 2015.
[109] O. Montenbruck, P. Steigenberger, and A. Hauschild, "Broadcast versus precise ephemerides: A multi-GNSS perspective," *GPS Solutions*, vol. 19, no. 2, pp. 321–333, 2015.
[110] L. Meng, J. Chen, J. Wang, and Y. Zhang, "Broadcast ephemerides for LEO augmentation satellites based on nonsingular elements," *GPS Solutions*, vol. 25, no. 4, p. 129, Oct. 2021.
[111] X. Xie, T. Geng, Q. Zhao, X. Liu, Q. Zhang, and J. Liu, "Design and validation of broadcast ephemeris for low Earth orbit satellites," *GPS Solutions*, vol. 22, no. 2, p. 54, Apr. 2018.
[112] X. Guo, L. Wang, W. Fu, Y. Suo, R. Chen, and H. Sun, "An optimal design of the broadcast ephemeris for LEO navigation augmentation systems," *Geo-Spatial Inf. Sci.*, vol. 25, no. 1, pp. 34–46, 2022.
[113] J. Yuan, S. Zhou, X. Hu, L. Yang, J. Cao, K. Li, and M. Liao, "Impact of attitude model, phase wind-up and phase center variation on precise orbit and clock offset determination of GRACE-FO and centispace-1," *Remote Sens.*, vol. 13, no. 13, p. 2636, Jul. 2021.
[114] K. Davies, Ed., *Ionospheric Radio*. London, U.K.: P. Peregrinus on Behalf of the Institution of Electrical Engineers, 1990.
[115] E. V. Appleton, "Wireless studies of the ionosphere," *Inst. Elect. Eng. Proc. Wireless Inst.*, vol. 7, no. 21, pp. 257–265, Sep. 1932.
[116] D. R. Hartree, "The propagation of electromagnetic waves in a refracting medium in a magnetic field," *Math. Proc. Cambridge Phil. Soc.*, vol. 27, no. 1, pp. 143–162, Jan. 1931.
[117] L. Marini-Pereira, L. F. D. Lourenço, J. Sousasantos, A. O. Moraes, and S. Pullen, "Regional ionospheric delay mapping for low-latitude environments," *Radio Sci.*, vol. 55, no. 12, pp. 1–12, Dec. 2020.
[118] J. Klobuchar, "Ionospheric time-delay algorithm for single-frequency GPS users," *IEEE Trans. Aerosp. Electron. Syst.*, vol. AES-23, no. 3, pp. 325–331, May 1987.
[119] B. Nava, P. Coïsson, and S. Radicella, "A new version of the NeQuick ionosphere electron density model," *J. Atmos. Sol.-Terr. Phys.*, vol. 70, no. 15, pp. 1856–1862, Dec. 2008.
[120] Y. Yuan, N. Wang, Z. Li, and X. Huo, "The BeiDou global broadcast ionospheric delay correction model (BDGIM) and its preliminary performance evaluation results," *Navigation*, vol. 66, no. 1, pp. 55–69, Jan. 2019.
[121] M. Hernàndez-Pajares, J. M. Juan, J. Sanz, R. Orus, A. Garcia-Rigo, J. Feltens, A. Komjathy, S. C. Schaer, and A. Krankowski, "The IGS VTEC maps: A reliable source of ionospheric information since 1998," *J. Geodesy*, vol. 83, no. 3, pp. 263–275, Mar. 2009.
[122] F. dos Santos Prol, P. de Oliveira Camargo, J. F. G. Monico, and M. T. de Assis Honorato Muella, "Assessment of a TEC calibration procedure by single-frequency PPP," *GPS Solutions*, vol. 22, p. 35, Apr. 2018.
[123] F. S. Prol, M. M. Hoque, and A. A. Ferreira, "Plasmasphere and topside ionosphere reconstruction using METOP satellite data during geomagnetic storms," *J. Space Weather Space Climate*, vol. 11, p. 5, Jan. 2021.
[124] Z. G. Elmas, M. Aquino, H. A. Marques, and J. F. G. Monico, "Higher order ionospheric effects in gnss positioning in the European region," *Ann. Geophys.*, vol. 29, pp. 1383–1399, Jan. 2011.
[125] A. W. Wernik, J. A. Secan, and E. J. Fremouw, "Ionospheric irregularities and scintillation," *Adv. Space Res.*, vol. 31, no. 4, pp. 971–981, 2003.
[126] N. Linty, A. Minetto, F. Dovis, and L. Spogli, "Effects of phase scintillation on the GNSS positioning error during the September 2017 storm at Svalbard," *Space Weather*, vol. 16, no. 9, pp. 1317–1329, 2018.
[127] E. J. Fremouw, R. L. Leadabrand, R. C. Livingston, M. D. Cousins, C. L. Rino, B. C. Fair, and R. A. Long, "Early results from the DNA wideband satellite experiment-complex-signal scintillation," *Radio Sci.*, vol. 13, no. 1, pp. 167–187, Jan. 1978.
[128] A. O. Moraes, E. Costa, M. A. Abdu, F. S. Rodrigues, E. R. de Paula, K. Oliveira, and W. J. A. Perrella, "The variability of low-latitude ionospheric amplitude and phase scintillation detected by a triple-frequency GPS receiver," *Radio Sci.*, vol. 52, no. 4, pp. 439–460, Apr. 2017.
[129] B. Li, H. Ge, M. Ge, L. Nie, Y. Shen, and H. Schuh, "LEO enhanced global navigation satellite system (LeGNSS) for real-time precise positioning services," *Adv. Space Res.*, vol. 63, no. 1, pp. 73–93, Jan. 2019.
[130] H. Ge, B. Li, L. Nie, M. Ge, and H. Schuh, "LEO constellation optimization for LEO enhanced global navigation satellite system (LeGNSS)," *Adv. Space Res.*, vol. 66, no. 3, pp. 520–532, Aug. 2020.
[131] *ITU Recommendation P.2040: Effects of Building Materials and Structures on Radiowave Propagation Above About 100 MHz*, document P.2040-2 (09/2021), ITU Recommendation, International Telecommunication Union, United Nations, 2021.
[132] Z. Bodnaar, Z. Herczku, J. Bearces, I. Papp, F. Som, B. G. Molnaar, and I. Frigyes, "A detailed experimental study of the LEO satellite to indoor channel characteristics," *Int. J. Wireless Inf. Netw.*, vol. 6, no. 2, pp. 79–91, 1999.
[133] A. Tkac and V. Wieser, "Channel estimation using measurement of channel impulse response," in *Proc. ELEKTRO*, May 2014, pp. 113–117.
[134] S. Lien, F. Choy, and M. Cherniakov, "Outdoor-to-indoor propagation modelling for LEO satellite communication systems," in *Proc. IEEE IEEE Region Annu. Conf. Speech Image Technol. Comput. Telecommun. (TENCON)*, vol. 1, Dec. 1997, pp. 105–108.
[135] T. Jost, W. Wang, U.-C. Fiebig, and F. Pérez-Fontán, "A wideband satellite-to-indoor channel model for navigation applications," *IEEE Trans. Antennas Propag.*, vol. 62, no. 10, pp. 5307–5320, Oct. 2014.
[136] T. Jost, W. Wang, A. Dammann, U.-C. Fiebig, M. Walter, and F. Schubert, "Satellite-to-indoor broadband channel measurements at 1.51 GHz and 5.2 GHz," in *Proc. 3rd Eur. Conf. Antennas Propag.*, Mar. 2009, pp. 2236–2240.
[137] H. Koivo and M. Elmusrati, *Systems Engineering in Wireless Communications*. Hoboken, NJ, USA: Wiley, 2009.
[138] M. Nakagami, "The *m*-distribution—A general formula of intensity distribution of rapid fading," in *Statistical Methods in Radio Wave Propagation*, W. Hoffman, Ed. New York, NY, USA: Pergamon, 1960, pp. 3–36.
[139] G. Gutt, D. Lawrence, S. Cobb, and M. O'Connor, "Recent PNT improvements and test results based on low Earth orbit satellites," in *Proc. Int. Tech. Meeting Inst. Navigat.*, Reston, VA, USA, Feb. 2018, pp. 570–577.
[140] T. G. R. Reid, B. Chan, A. Goel, K. Gunning, B. Manning, J. Martin, A. Neish, A. Perkins, and P. Tarantino, "Satellite navigation for the age of autonomy," in *Proc. IEEE/ION Position, Location Navigat. Symp. (PLANS)*, Apr. 2020, pp. 342–352.

[141] Y. T. J. Morton, F. Diggelen, J. J. Spilker, B. W. Parkinson, S. Lo, and G. Gao, Eds., *Position, Navigation, and Timing Technologies in the 21st Century*, vol. 1. Hoboken, NJ, USA: Wiley, 2020.

[142] L. Wang, R. Chen, D. Li, G. Zhang, X. Shen, B. Yu, C. Wu, S. Xie, P. Zhang, M. Li, and Y. Pan, "Initial assessment of the LEO based navigation signal augmentation system from luojia-1A satellite," *Sensors*, vol. 18, no. 11, p. 3919, Nov. 2018.

[143] F. Farhangian and R. Landry, "Multi-constellation software-defined receiver for Doppler positioning with LEO satellites," *Sensors*, vol. 20, no. 20, p. 5866, Oct. 2020.

[144] J. Khalife, M. Neinavaie, and Z. Z. Kassas, "The first carrier phase tracking and positioning results with starlink LEO satellite signals," *IEEE Trans. Aerosp. Electron. Syst.*, vol. 58, no. 2, pp. 1487–1491, Apr. 2022.

[145] J. J. Khalife and Z. M. Kassas, "Receiver design for Doppler positioning with LEO satellites," in *Proc. IEEE Int. Conf. Acoust., Speech Signal Process. (ICASSP)*, May 2019, pp. 5506–5510.

[146] M. L. Psiaki, "Navigation using carrier Doppler shift from a LEO constellation: TRANSIT on steroids," *Navigation*, vol. 68, no. 3, pp. 621–641, Sep. 2021.

[147] P. A. Iannucci and T. E. Humphreys, "Economical fused LEO GNSS," in *Proc. IEEE/ION Position, Location Navigat. Symp. (PLANS)*, Apr. 2020, pp. 426–443.

[148] Z. Tan, H. Qin, L. Cong, and C. Zhao, "Positioning using IRIDIUM satellite signals of opportunity in weak signal environment," *Electronics*, vol. 9, no. 1, p. 37, Dec. 2019.

[149] L. Cheng, Y. Dai, W. Guo, and J. Zheng, "Structure and performance analysis of signal acquisition and Doppler tracking in LEO augmented GNSS receiver," *Sensors*, vol. 21, no. 2, p. 525, Jan. 2021.

[150] S. Thompson, S. Martin, and D. Bevly, "Single differenced Doppler positioning with low Earth orbit signals of opportunity and angle of arrival estimation," in *Proc. Int. Tech. Meeting Inst. Navigat.*, Feb. 2021, pp. 497–509.

[151] Z. M. Kassas, J. J. Khalife, and J. J. Morales, "New-age satellite-based navigation–STAN: Simultaneous tracking and navigation with LEO satellite signals," *Inside GNSS Mag.*, vol. 14, no. 4, pp. 56–65, 2019.

[152] R. Santerre, L. Pan, C. Cai, and J. Zhu, "Single point positioning using GPS, GLONASS and BeiDou satellites," *Positioning*, vol. 5, no. 4, pp. 107–114, 2014.

[153] K. Su, S. Jin, and M. Hoque, "Evaluation of ionospheric delay effects on multi-GNSS positioning performance," *Remote Sens.*, vol. 11, no. 2, p. 171, Jan. 2019.

[154] J. Geng, Q. Wen, Q. Zhang, G. Li, and K. Zhang, "GNSS observable-specific phase biases for all-frequency PPP ambiguity resolution," *J. Geodesy*, vol. 96, no. 2, p. 11, Feb. 2022.

[155] M. Bakuła, "Network code DGPS positioning and reliable estimation of position accuracy," *Surv. Rev.*, vol. 42, no. 315, pp. 82–91, Jan. 2010.

[156] D. Alves, L. Dalbelo, J. Monico, and M. Shimabukuro, "First Brazilian real time network DGPS through the internet: Development, application and availability analyses," *J. Geodetic Sci.*, vol. 2, no. 1, pp. 1–7, Jan. 2012.

[157] D. B. M. Alves and J. F. G. Monico, "GPS/VRS positioning using atmospheric modeling," *GPS Solutions*, vol. 15, no. 3, pp. 253–261, Jul. 2011.

[158] L. García-Asenjo, S. Baselga, C. Atkins, and P. Garrigues, "Development of a submillimetric GNSS-based distance meter for length metrology," *Sensors*, vol. 21, no. 4, p. 1145, Feb. 2021.

[159] F. Zhu, T. Ba, Y. Zhang, X. Gao, and J. Wang, "Terminal location method with NLOS exclusion based on unsupervised learning in 5G-LEO satellite communication systems," *Int. J. Satell. Commun. Netw.*, vol. 38, no. 5, pp. 425–436, 2020. [Online]. Available: https://onlinelibrary.wiley.com/doi/pdf/10.1002/sat.1346

[160] J. Yan, C. C. J. M. Tiberius, G. J. M. Janssen, P. J. G. Teunissen, and G. Bellusci, "Review of range-based positioning algorithms," *IEEE Aerosp. Electron. Syst. Mag.*, vol. 28, no. 8, pp. 2–27, Aug. 2013.

[161] Y. T. Chan and K. C. Ho, "A simple and efficient estimator for hyperbolic location," *IEEE Trans. Signal Process.*, vol. 42, no. 8, pp. 1905–1915, Aug. 1994.

[162] G. Shen, R. Zetik, and R. S. Thoma, "Performance comparison of TOA and TDOA based location estimation algorithms in LOS environment," in *Proc. 5th Workshop Positioning, Navigat. Commun.*, Mar. 2008, pp. 71–78.

[163] J. Yan, C. C. J. M. Tiberius, P. J. G. Teunissen, G. Bellusci, and G. J. M. Janssen, "A framework for low complexity least-squares localization with high accuracy," *IEEE Trans. Signal Process.*, vol. 58, no. 9, pp. 4836–4847, Sep. 2010.

[164] R. E. Kalman, "A new approach to linear filtering and prediction problems," *J. Basic Eng.*, vol. 82, no.1, pp. 35–45, May 1960.

[165] R. Faragher, "Understanding the basis of the Kalman filter via a simple and intuitive derivation [lecture notes]," *IEEE Signal Process. Mag.*, vol. 29, no. 5, pp. 128–132, Sep. 2012.

[166] Y. Bar-Shalom, "Recursive tracking algorithms: From the Kalman filter to intelligent trackers for cluttered environment," in *Proc. IEEE Int. Conf. Control Appl. (ICCON)*, Apr. 1989, pp. 675–680.

[167] J. Hartikainen, A. Solin, and S. Särkkä, *Optimal Filtering With Kalman Filters and Smoothers—A Manual for MATLAB Toolbox EKF/UKF*. Espoo, Finland: Aalto Univ., 2011.

[168] Y. Bar-Shalom, X. R. Li, and T. Kirubarajan, *Estimation With Applications to Tracking and Navigation*. Hoboken, NJ, USA: Wiley, 2001.

[169] S. J. Julier and J. K. Uhlmann, "Unscented filtering and nonlinear estimation," *Proc. IEEE*, vol. 92, no. 3, pp. 401–422, Mar. 2004.

[170] F. Gustafsson, F. Gunnarsson, N. Bergman, U. Forssell, J. Jansson, R. Karlsson, and P.-J. Nordlund, "Particle filters for positioning, navigation, and tracking," *IEEE Trans. Signal Process.*, vol. 50, no. 2, pp. 425–437, Feb. 2002.

[171] J. Elfring, E. Torta, and R. van de Molengraft, "Particle filters: A hands-on tutorial," *Sensors*, vol. 21, no. 2, p. 438, Jan. 2021.

[172] V. Indelman, S. Williams, M. Kaess, and F. Dellaert, "Information fusion in navigation systems via factor graph based incremental smoothing," *Robot. Auto. Syst.*, vol. 61, no. 8, pp. 721–738, Aug. 2013.

[173] T. Pfeifer and P. Protzel, "Expectation-maximization for adaptive mixture models in graph optimization," in *Proc. Int. Conf. Robot. Autom. (ICRA)*, May 2019, pp. 3151–3157.

[174] J. Kennedy and R. Eberhart, "Particle swarm optimization," in *Proc. Int. Conf. Neural Netw. (ICNN)*, vol. 4, Nov./Dec. 1995, pp. 1942–1948.

[175] H. Wu, J. Liu, Z. Dong, and Y. Liu, "A hybrid mobile node localization algorithm based on adaptive MCB-PSO approach in wireless sensor networks," *Wireless Commun. Mobile Comput.*, vol. 2020, pp. 1–17, Jun. 2020, Art. no. e3845407.

[176] M. Neinavaie, J. Khalife, and Z. M. Kassas, "Acquisition, Doppler tracking, and positioning with starlink LEO satellites: First results," *IEEE Trans. Aerosp. Electron. Syst.*, vol. 58, no. 3, pp. 2606–2610, Jun. 2022.

[177] F. Farhangian, H. Benzerrouk, and R. Landry, "Opportunistic in-flight INS alignment using LEO satellites and a rotatory IMU platform," *Aerospace*, vol. 8, no. 10, p. 280, Sep. 2021.

[178] M. Elsanhoury, J. Koljonen, P. Välisuo, M. Elmusrati, and H. Kuusniemi, "Survey on recent advances in integrated GNSSs towards seamless navigation using multi-sensor fusion technology," in *Proc. 34th Int. Tech. Meeting Satell. Division Inst. Navigat. (ION GNSS+)*, Sep. 2021, pp. 2754–2765.

[179] M. Vemula, M. F. Bugallo, and P. M. Djuric, "Performance comparison of Gaussian-based filters using information measures," *IEEE Signal Process. Lett.*, vol. 14, no. 12, pp. 1020–1023, Dec. 2007.

[180] Z. Luan, Z. Li, and Y. Li, "Research on carrier tracking algorithm of low earth orbit satellite based on particle filter," *Proc. SPIE*, vol. 11373, pp. 839–846, Jan. 2020.

[181] R. Awadhiya, "Particle filter based track before detect method for space surveillance radars," in *Proc. IEEE Radar Conf. (RadarConf)*, Mar. 2022, pp. 1–6.

[182] W. Wen, T. Pfeifer, X. Bai, and L. T. Hsu, "Factor graph optimization for GNSS/INS integration: A comparison with the extended Kalman filter," *J. Inst. Navigat.*, vol. 68, no. 2, pp. 315–331, 2020.

[183] N. Sunderhauf and P. Protzel, "Towards robust graphical models for GNSS-based localization in urban environments," in *Proc. Int. Multi-Conf. Syst., Sygnals Devices*, Mar. 2012, pp. 1–6.

[184] V. Indelman, S. Williams, M. Kaess, and F. Dellaert, "Factor graph based incremental smoothing in inertial navigation systems," in *Proc. 15th Int. Conf. Inf. Fusion*, Jul. 2012, pp. 2154–2161.

[185] R. Eberhart and J. Kennedy, "A new optimizer using particle swarm theory," in *Proc. 6th Int. Symp. Micro Mach. Hum. Sci. (MHS)*, 1995, pp. 39–43.

[186] D. Zhao, C. Cai, and L. Li, "A binary discrete particle swarm optimization satellite selection algorithm with a queen informant for multi-GNSS continuous positioning," *Adv. Space Res.*, vol. 68, no. 9, pp. 3521–3530, Nov. 2021.

[187] E. Wang, C. Jia, G. Tong, P. Qu, X. Lan, and T. Pang, "Fault detection and isolation in GPS receiver autonomous integrity monitoring based on chaos particle swarm optimization-particle filter algorithm," *Adv. Space Res.*, vol. 61, no. 5, pp. 1260–1272, Mar. 2018.

[188] X. Guo, N. Ansari, F. Hu, Y. Shao, N. R. Elikplim, and L. Li, "A survey on fusion-based indoor positioning," *IEEE Commun. Surveys Tuts.*, vol. 22, no. 1, pp. 566–594, 1st Quart., 2020.
[189] P. Srinivas and A. Kumar, "Overview of architecture for GPS-INS integration," in *Proc. Recent Develop. Control, Autom. Power Eng. (RDCAPE)*, Oct. 2017, pp. 433–438.
[190] P. A. Iannucci and T. E. Humphreys, "Fused low-earth-orbit GNSS," *IEEE Trans. Aerosp. Electron. Syst.*, Jun. 6, 2022, doi: 10.1109/TAES.2022.3180000.
[191] Z. Kassas, J. Morales, and J. Khalife, "New-age satellite-based navigation STAN: Simultaneous tracking and navigation with leo satellite signals," *Inside GNSS*, vol. 14, no. 4, 2019.
[192] L. You, K.-X. Li, J. Wang, X. Gao, X.-G. Xia, and B. Ottersten, "Massive MIMO transmission for LEO satellite communications," *IEEE J. Sel. Areas Commun.*, vol. 38, no. 8, pp. 1851–1865, Aug. 2020.
[193] Y. Zhang, Y. Wu, A. Liu, X. Xia, T. Pan, and X. Liu, "Deep learning-based channel prediction for LEO satellite massive MIMO communication system," *IEEE Wireless Commun. Lett.*, vol. 10, no. 8, pp. 1835–1839, Aug. 2021.
[194] *Systems Tool Kit (STK) by AGI*, Analytical Graphics, (AGI), Exton, PA, USA, 2022.
[195] S. P. Hughes, "General mission analysis tool (GMAT)," NASA, Washington, DC, USA, Tech. Rep., 2016.
[196] D. J. Conway and S. P. Hughes, "The general mission analysis tool (GMAT): Current features and adding custom functionality," in *Proc. Int. Conf. Astrodyn. Tools Techn. (ICATT)*, 2010, pp. 1–8.
[197] J. Galán-Vioque, R. Vázquez, E. Carrizosa, C. Vera, F. Perea, and F. Martín, "Towards a visual tool for swath acquisition planning in multiple-mission EoSs," in *Proc. IWPSS Workshop*, 2011, pp. 1–8.
[198] P. Truchly and J. Cervienka, "Simple visualization tool for analysis of satellite orbits and constellations," in *Proc. Int. Conf. Emerg. eLearning Technol. Appl. (ICETA)*, Nov. 2016, pp. 359–364, doi: 10.1109/ICETA.2016.7802101.
[199] *SaVoir Multi-Satellite Swath Planner*, Taitus Software, Rome, Italy, 2022.
[200] S. Jaeckel, L. Raschkowski, K. Börner, and L. Thiele, "QuaDRiGa: A 3-D multi-cell channel model with time evolution for enabling virtual field trials," *IEEE Trans. Antennas Propag.*, vol. 62, no. 6, pp. 3242–3256, Jun. 2014.
[201] S. Jaeckel, L. Raschkowski, K. Börner, and L. Thiele, "QuaDRiGa: A 3-D multi-cell channel model with time evolution for enabling virtual field trials," *IEEE Trans. Antennas Propag.*, vol. 62, no. 6, pp. 3242–3256, 2014, doi: 10.1109/TAP.2014.2310220.
[202] S. Jaeckel, L. Raschkowski, and L. Thieley, "A 5G-NR satellite extension for the QuaDRiGa channel model," in *Proc. Joint Eur. Conf. Netw. Commun. 6G Summit (EuCNC/6G Summit)*, Jun. 2022, pp. 142–147.
[203] X. Ren, J. Zhang, J. Chen, and X. Zhang, "Global ionospheric modeling using multi-GNSS and upcoming LEO constellations: Two methods and comparison," *IEEE Trans. Geosci. Remote Sens.*, vol. 60, pp. 1–15, 2022.
[204] S. Xiong, F. Ma, X. Ren, J. Chen, and X. Zhang, "LEO constellation-augmented multi-GNSS for 3D water vapor tomography," *Remote Sens.*, vol. 13, no. 16, p. 3056, Aug. 2021.
[205] A. Ojala, "Business models and opportunity creation: How IT entrepreneurs create and develop business models under uncertainty," *Inf. Syst. J.*, vol. 26, no. 5, pp. 451–476, Sep. 2016.
[206] M. Vidmar, A. Rosiello, and O. Golra, "Resilience of new space firms in the United Kingdom during the early stages of COVID-19 crisis: The case for strategic agility," *New Space*, vol. 8, no. 4, pp. 172–178, Dec. 2020.

F. S. PROL received the Ph.D. degree in cartographic sciences from São Paulo State University (UNESP), Brazil, with a focus on geodetic remote sensing and geodetic positioning, in 2019. He has been working at the Finnish Geospatial Research Institute (FGI), since 2021. His research interests include ionospheric modeling, GNSS positioning, and data assimilation.

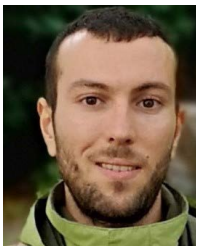

R. MORALES FERRE received the B.Sc. degree in telecommunication systems engineering and the M.Sc. degree in telecommunication engineering from the Universitat Autonoma de Barcelona (UAB), in 2016 and 2018, respectively. He is currently pursuing the double Ph.D. degree with Tampere University (TAU) and UAB. He worked as a Research Assistant with the Signal Processing for Communications & Navigation (SPCOMNAV) Group, UAB, until 2018. In 2018, he received a TAU rector's grant, which partially finances his Ph.D. studies. He is also involved as a Ph.D. Researcher in EU and Academy of Finland funded projects. His current research interests include GNSS security and integrity, signal processing with applications to communications and navigation, and positioning by means of GNSS and alternative positioning methods, such as cellular networks or LEO constellations and array signal processing.

Z. SALEEM (Graduate Student Member, IEEE) received the bachelor's degree in mechatronics engineering from NUST, Pakistan, and the double master's degree in space science and technology with space robotics as a major from Erasmus Mundus Program, Aalto University, Finland, and the Luleå University of Technology, Sweden. She is currently pursuing the Ph.D. degree with the School of Electrical Engineering, Aalto University, working on distributed space systems. Her area of expertises are guidance, navigation, and control with experience across aerospace and robotics.

P. VÄLISUO received the M.Sc. (Tech.) degree in computer science from the Tampere University of Technology, Finland, in 1996, and the D.Sc. (Tech.) degree in automation technology from the University of Vaasa, Finland, in 2011. He has worked for ten year's in telecommunications industry before establishing a research career with the University of Vaasa, where he is currently working as an Associate Professor (a tenure Track), sustainable automation with the School of Technology and Innovation Management. He has authored and coauthored 27 peer-reviewed and more than ten other scientific publications. His research interests include ML, the IoT, positioning methods, and other technologies relevant to industrial automation.

C. PINELL received the B.Sc. degree in physics from the University of Bonn, Germany, in 2018, and the double M.Sc. (Tech.) degree in space science and technology from Aalto University, Finland, and the Luleå University of Technology, Sweden, in 2021. She is currently conducting research at the Finnish Geospatial Research Institute (FGI). Her research interests include space science and instrumentation, resilient PNT, and receiver technologies.

E. S. LOHAN (Senior Member, IEEE) received the M.Sc. degree in electrical engineering from the Polytechnics University of Bucharest, Romania, in 1997, the D.E.A. degree (French equivalent of master) in econometrics with the Ecole Polytechnique, Paris, France, in 1998, and the Ph.D. degree in telecommunications from the Tampere University of Technology, in 2003. She is currently a Professor at Tampere University (TAU), Finland, where she is also a Professor at the Electrical Engineering Unit, and the Coordinator of the MSCA EU "A-WEAR" network. Her current research interests include GNSS, LEO-PNT, wireless location techniques, wearable computing, and privacy-aware positioning solutions.

M. ELSANHOURY (Graduate Student Member, IEEE) received the B.Sc. degree in telecommunications engineering from Alexandria University, Egypt, in 2013, and the M.Sc. (Tech.) degree in telecommunications engineering from the University of Vaasa, Finland, in 2018, where he is currently pursuing the Ph.D. degree in computer science. From 2017 to 2018, he worked as a Research Assistant at the University of Vaasa. In Spring 2017, he worked as an Autonomous Robots Lecturer at the Swedish NOVIA University of Applied Sciences. Recently in 2021, he conducted a two-month research visit to American University in Cairo (AUC) to exchange research ideas around UWB and LEO positioning. His current research interests include ubiquitous indoor positioning systems, ultra-wideband (UWB) indoor localization, low-earth orbit (LEO) satellites for positioning, multi-sensor fusion technologies, Kalman filters, and machine learning algorithms.

M. ELMUSRATI (Senior Member, IEEE) received the B.Sc. and M.Sc. degrees (Hons.) in electrical and electronic engineering from the University of Benghazi, Libya, in 1991 and 1995, respectively, and the Licentiate of Science degree (Hons.) in technology and the Doctor of Science (D.Sc.) degree in automation and control engineering (technology) from Aalto University, Finland, in 2002 and 2004, respectively. Currently, he is a Full Professor in communication, automation, and digitalization at the School of Technology and Innovations—University of Vaasa, Finland. He has published about 150 papers, books, and book chapters. His research interests include wireless communications, artificial intelligence, machine learning, biotechnology, big data analysis, stochastic systems, and game theory. He is an Active Member in different scientific societies, such as a member of the Society of Industrial and Applied Mathematics (SIAM) and a member of Finnish Automation Society.

S. ISLAM received the M.Sc. (Tech.) degree (Hons.) from Tampere University (TAU), Finland, in 2019, where he is currently pursuing the Ph.D. degree. He is also a Research Scientist at the Finnish Geospatial Research Institute (FGI-NLS). He is a member of the Resilient Position, Navigation, and Timing Group, Department of Navigation and Positioning, FGI-NLS. He is involved in research projects on GNSS receiver development and validation, timing algorithms, maritime navigation, LEO-PNT, GNSS jamming, and spoofing. He is one of the key people in the implementation of the GPS L5 solution in FGI-GSRx. His research interests include GNSS signal processing, resilient software-defined radio (SDR) development, satellite-based augmentation systems (SBAS), and 5G new radio (NR).

K. ÇELIKBILEK received the B.Sc. (Tech.) degree in electrical and electronics engineering from Bilkent University, in 2018, and the M.Sc. (Tech.) degree in robotics and artificial intelligence from Tampere University, in 2020, where he is currently pursuing the Ph.D. degree in computing and electrical engineering. His research interests include deep learning, reinforcement learning, multi-objective optimization, satellite communication, and robotics.

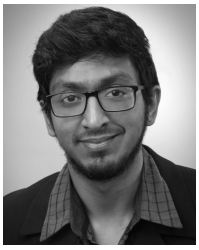

K. SELVAN received the B.S. degree in electronics and communication engineering from Anna University, India, in 2012, and the M.S. degree in communications and systems engineering from the University of Vaasa, Finland, in 2020, where he is currently pursuing the Ph.D. degree in automation technology. From 2018 to 2020, he was a Research Assistant at Digital Economy Research Platform, University of Vaasa, where he is currently a Project Researcher at Digital Economy Research Platform. His research interests include GNSS technologies, LEO-PNT, satellite-data analysis, machine learning, satellite communication, and smart devices.

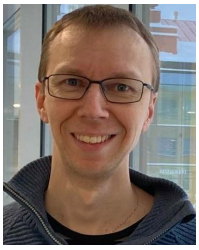

J. YLIAHO received the M.Sc. (Tech.) degree in electrical engineering from the Tampere University of Technology, in 2008. He is currently pursuing the Ph.D. degree with the University of Vaasa, Finland. He is also a Laboratory Engineer with the University of Vaasa. His current research interests include space-based signals of opportunity for PNT and related projects at Digital Economy Research Platform, University of Vaasa.

K. RUTLEDGE received the B.A. and B.S. degrees in environmental and biological sciences from Lenoir-Rhyne University, Hickory, NC, USA, in 1978, and the M.Sc. degree in marine systems ecology and biostatistics from Old Dominion University, Norfolk, VA, USA, in 1982. He is currently the Research Program Manager of Space and the Project Manager of Digital Economy Research Platform, University of Vaasa, Vaasa, Finland. He has been working with atmospheric acoustics, satellite instrument algorithm development and surface observation systems as a NASA Contractor in the USA. He worked as a Site Scientist for several surface observation networks, including NASA's AERONET, MPLNET, and the WMO's baseline surface radiation network. This work included instrumenting an offshore observation platform to support components of NASA's Clouds and the Earth's Radiant Energy System program (in the ocean environment). Recently, he has developed or help develop projects associated with wind, ice and space in Scandinavia.

A. OJALA received the Ph.D. degree in economics from the University of Jyväskylä. He is currently a Professor in international business with the School of Marketing and Communication, University of Vaasa, Finland. He is also an Adjunct Professor in software business at Tampere University, Finland. His articles have been published in *Information Systems Journal*, *Journal of World Business*, *Journal of Systems and Software*, *Journal of Cleaner Production*, IEEE SOFTWARE, *IT Professional*, and among other academic venues. His research interests include global digital business, international entrepreneurship, and business models.

L. FERRANTI received the B.Sc. (Tech.) and M.Sc. (Tech.) degrees in electrical engineering from the Tampere University of Technology, in 2018 and 2019, respectively. He is currently pursuing the Ph.D. degree in computer science with the University of Vaasa. His current research interests include computational mathematics and its applications to engineering domains and applying algebraic geometry methods to positioning problems.

J. PRAKS (Member, IEEE) received the B.Sc. degree in physics from the University of Tartu, Estonia, in 1996, and the D.Sc. (Tech.) degree in space technology and remote sensing from Aalto University, Espoo, Finland, in 2012. He is currently an Assistant Professor in electrical engineering with the Department of Electronics and Nanoengineering, School of Electrical Engineering, Aalto University. He has been working with microwave remote sensing, scattering modeling, microwave radiometry, hyperspectral imaging and with advanced SAR techniques, such as polarimetry, interferometry, polarimetric interferometry, and tomography. One of most visited topic in his research is remote sensing of boreal forest. Since 2009, he has been taken interest in emerging nanosatellite technology. He led project which produced two first Finnish satellites. He has been involved also in spinning off several companies in the field of satellite remote sensing. His research team is a member or the Finnish Centre of Excellence in Research of Sustainable Space and he is a Principal Investigator of several small satellite missions. He is an Active Member of scientific community, a member of Finnish National Committee of COSPAR, the Chairperson of Finnish National Committee of URSI, and the chair and the co-chair of many national and international conferences.

M. Z. H. BHUIYAN is currently a Research Professor at the Department of Navigation and Positioning, Finnish Geospatial Research Institute. He has been also working as a Technical Expert of the EU Agency for the Space Program (EUSPA) in H2020 project reviewing and proposal evaluation. His research interests include multi-GNSS receiver development, PNT robustness and resilience, and seamless positioning. He is actively involved in teaching GNSS related courses in Finnish universities and other training schools.

S. KAASALAINEN is currently a Professor and the Head of the Department of Navigation and Positioning, FGI of the National Land Survey. Her research interests include resilient PNT, situational awareness, and optical sensors. She also has research experience in Lidar remote sensing, sensor development, and astronomy.

H. KUUSNIEMI (Member, IEEE) received the M.Sc. degree (Hons.) in information technology and the Ph.D. degree from the Tampere University of Technology, Finland, in 2002 and 2005, respectively. She is currently the Director of the Digital Economy Research Platform and a Professor in computer science at the University of Vaasa, a Research Professor at the Finnish Geospatial Research Institute, National Land Survey of Finland, and an Adjunct Professor in satellite navigation at Tampere University and Aalto University, Finland. She has more than 20 year's of experience in research and development of positioning technologies and has held many significant positions of trust and expertise in the global scientific navigation community. Part of her Ph.D. research was conducted at the Department of Geomatics Engineering, University of Calgary, Canada. She was a member of the Research Council for Natural Sciences and Engineering at the Academy of Finland (2019–2021) and a Visiting Scholar at the GPS Laboratory, Stanford University, in 2017. Her research interests include global navigation satellite systems, especially reliability, estimation and data fusion, mobile precision positioning with applications, indoor localization, and opportunities of PNT in new space.